2009 ANNUAL REPORT
FUSION RESEARCH CENTER
GEORGIA INSTITUTE OF TECHNOLOGY
ATLANTA, GA 30332-0425

RESEARCH SUMMARY

During 2009, research focused on i) interpretation of plasma edge experiments in DIII-D (DoE Grant DE-FG02-99-ER54538), ii) further analysis of the SABR fusion-fission hybrid actinide burner reactor concept developed at Georgia Tech (DoE Grant DE-SC0002202), and iii) related topics in theoretical/computation plasma physics. This work and publication/presentations based on it are summarized in this report.

FRC FACULTY & STUDENTS

Faculty---W. M. Stacey (NRE), B. Petrovic (NRE), S. M. Ghiaasiaan (ME), J. Schwartz (MSE)
Graduate Students---C. Bae, Z. W. Friis, J.-P. Floyd, C. M. Sommer, C. Stuart, T. S. Sumner (NRE)
Undergraduate Students---R. Lober (NRE), L. Zhou (Phys)

COLLABORATION

Faculty and students in the Georgia Tech Fusion Research Center collaborate in the analysis and interpretation of plasma physics experiments with researchers from General Atomics, Lawrence Livermore National Laboratory, Oak Ridge National Laboratory and other research institutions as a member of the DIII-D National Tokamak Facility. This includes participation in the DIII-D H-Mode Edge Pedestal (HEP) activity which is comparing various codes and methods for internpreting transport in the tokamak edge pedestal.

The Georgia Tech FRC joined an ongoing study at the KIT—Karlsruhe Institute of Technology and CEA—Cadarache of various scenarios for the deployment of actinide burner reactors to support an expansion of nuclear power in Europe. The present study, including critical and accelerator-driven (ADS) fast burner reactors is being expanded to include the SABR fusion-fission hybrid burner reactor concept developed at Georgia Tech.

TECHNICAL PRESENTATIONS

1. "Interpretation of neutral fueling and pedestal recycling", DIII- D Science Mtg, San Diego, July,2009; W. M. Stacey
2. "Particle pinches and diffusion coefficients in the edge pedestal of DIII-D", DIII-D Science Mtg., San Diego, July, 2009; W. M. Stacey.

3. "Fusion-Fission Hybrids", seminar, General Atomics, San Diego, August, 2009; W. M. Stacey.
4. "Analysis of pedestal transport", H-Mode Workshop, Princeton, NJ, September 30, 2009; J. D. Callen, R. J. Groebner, L. W. Owen, J. M Canik A. Y. Pankin, T. Rafiq, T. D. Rognlien and W. M. Stacey
5. "Effect of a pinch on inferred particle diffusion coefficients in the pedestal", ITPA Pedestal Group Meeting, Princeton, NJ, October 5, 2009; J. Callen, R. Groebner, J. Canik, L. Owen, A. Pankin, T. Rafiq, T. Rognlien and W. Stacey.
6. "SABR—Subcritical Advanced Burner Reactor", DoE ReNeW Workshop on Fusion-Fission Hybrids, Gaithersburg, MD, Sept. 30-Oct.2, 2009; W. M. Stacey.
7. "SABR Fuel Cycle", DoE ReNeW Workshop on Fusion-Fission Hybrids, Gaithersburg, MD, Sept. 30-Oct.2, 2009; W. M. Stacey, C. M.Sommer and B. Petrovic.
8. "SABR Dynamic Safety Analysis", DoE ReNeW Workshop on Fusion-Fission Hybrids, Gaithersburg, MD, Sept. 30-Oct.2, 2009; W. M. Stacey, T. S. Sumner and S. M. Ghiaasiaan.
9. "SABR Reactor Core and Tritium Breeding Blanket" DoE ReNeW Workshop on Fusion-Fission Hybrids, Gaithersburg, MD, Sept. 30-Oct.2, 2009; W. M. Stacey.
10. "Analysis of neutral recycling fueling of the DIII-D edge pedestal", APS-DPP, Atlanta, November, 2009; Z. W. Friis, W. M. Stacey, A. W. Leonard and M. Rensink.
11. "Generalized diffusion theory calculations of the edge pedestal density profiles", APS-DPP, Atlanta, November, 2009; J.-P. Floyd and W. M. Stacey.
12. "Analysis of particle transport in DIII-D H-mode plasma with a generalized pinch-diffusion model**,"** APS-DPP, Atlanta, November, 2009; L.W. Owen, R.J. Groebner, J.D. Callen, W. M. Stacey, and X. Bonnin.
13. "Dynamical Safety Analysis of the SABR Fusion-Fission Hybrid Reactor", APS-DPP, Atlanta, November, 2009; T. S. Sumner,W. M. Stacey, M. S. Ghiaassian.
14. "Analysis of pedestal transport", APS-DPP, Atlanta, November, 2009; J.D. Callen, R.J. Groebner, T.H. Osborne, J.M. Canik, L.W. Owen, A. Pankin, T. Rafiq, T.D. Rognlien and W. M. Stacey.
15. "Nuclear fuel cycle analysis of the SABR fusion-fission hybrid transmutation reactor", APS-DPP, Atlanta, November, 2009; C. M. Sommer, W. M. Stacey and B. Petrovick.
16. "Evaluation of particle pinch and diffusion coefficients in the edge pedestalof DIII-D H-mode discharges", APS-DPP, Atlanta, November, 2009; W. M. Stacey and R. J. Groebner.
17. "SABR—A fusion-fission hybrid reactor for the transmutation of spent nuclear fuel", APS-DPP, Atlanta, November, 2009; W. M. Stacey.
18. "The SABR Fusion-Fission Concept", Fusion Power Assocs. Annual Meeting, December, 2009; W. M. Stacey.

PEER-REVIEWED PAPERS

1. "An investigation of some effects of drifts and magnetic field direction in the scrape-off layer and divertor of tokamak plasmas", Phys. Plasmas, 16, 042502 (2009); W. M. Stacey.
2. "Effect on the divertor and scrape-off layer plasma properties of the distribution of power and particle influxes from the core", Phys. Plasmas, 16, 032506 (2009); W. M. Stacey.
3. "Georgia Tech Studies of Sub-Critical Advanced Burner Reactors with a D-T Fusion Tokamak Neutron Source for the Transmutation of Spent Nuclear Fuel", J. Fusion Energy 38, 328 (2009); W. M. Stacey.
4. "Rotation velocities in the plasma edge driven viscously by scrape-off layer flows", Phys. Plasmas 16, 062505 (2009); W. M. Stacey.
5. "Representation of the plasma fluid equations in Miller analytical flux surface coordinates", Phys. Plasmas 16, 082501 (2009); W. M. Stacey and C. Bae.
6. "Analysis of neutral particle recycling and pedestal fueling in an H-mode DIII-D discharge", Phys. Plasmas, submitted (2009); Z. Friis, W. M. Stacey, A. W. Leonard and M. Rensink.
7. "Interpretation of particle pinches and diffusion coefficients in the edge pedestal of DIII-D plasmas", Phys. Plasmas, accepted (2009); W. M. Stacey and R. J. Groebner.
8. "DIII-D research in support of ITER", Nucl. Fusion 49, 104008 (2009); E. J. Strait and the DIII-D Team.
9. "Analysis of pedestal transport", Nucl. Fusion, submitted (2009); J. D. Callen, R. J. Groebner, T. H. Osborne, J. M. Canik, L. W. Owen, A. Y. Pankin, T. Rafiq, T. D. Rognlien and W. M. Stacey.
10. C. M. Sommer, W. M. Stacey and B. Petrovic, "Fuel Cycle Analysis of the SABR Subcritical Transmutation Reactor Concept", *Nuclear Technol.*, submitted (2009).
11. T. S. Sumner, W. M. Stacey and S. M. Ghiaasiaan, "Dynamic Safety Analysis of the SABR Subcritical Transmutation Reactor Concept", *Nuclear Technol.*, submitted (2009).

TECHNICAL SUMMARIES

Analysis of neutral particle recycling and pedestal fueling in an H-mode DIII-D discharge

Z. W. Friis & W. M. Stacey, Georgia Tech
A. W. Leonard, General Atomics,
M. E. Rensink, Lawrence Livermore National Laboratory

November, 2009

INTRODUCTION

- Experimental ion fluxes to the wall and UEDGE calculations of background edge plasma parameters and recombination rates exist for several DIII-D shots from the work of Leonard, et al.
- The 2D GTNEUT neutral transport code has been modified to accept geometric and background plasma input from UEDGE by Friis, Rognlien, et al.
- This allows a detailed analysis of neutral particle recycling and fueling in a DIII-D H-mode discharge.

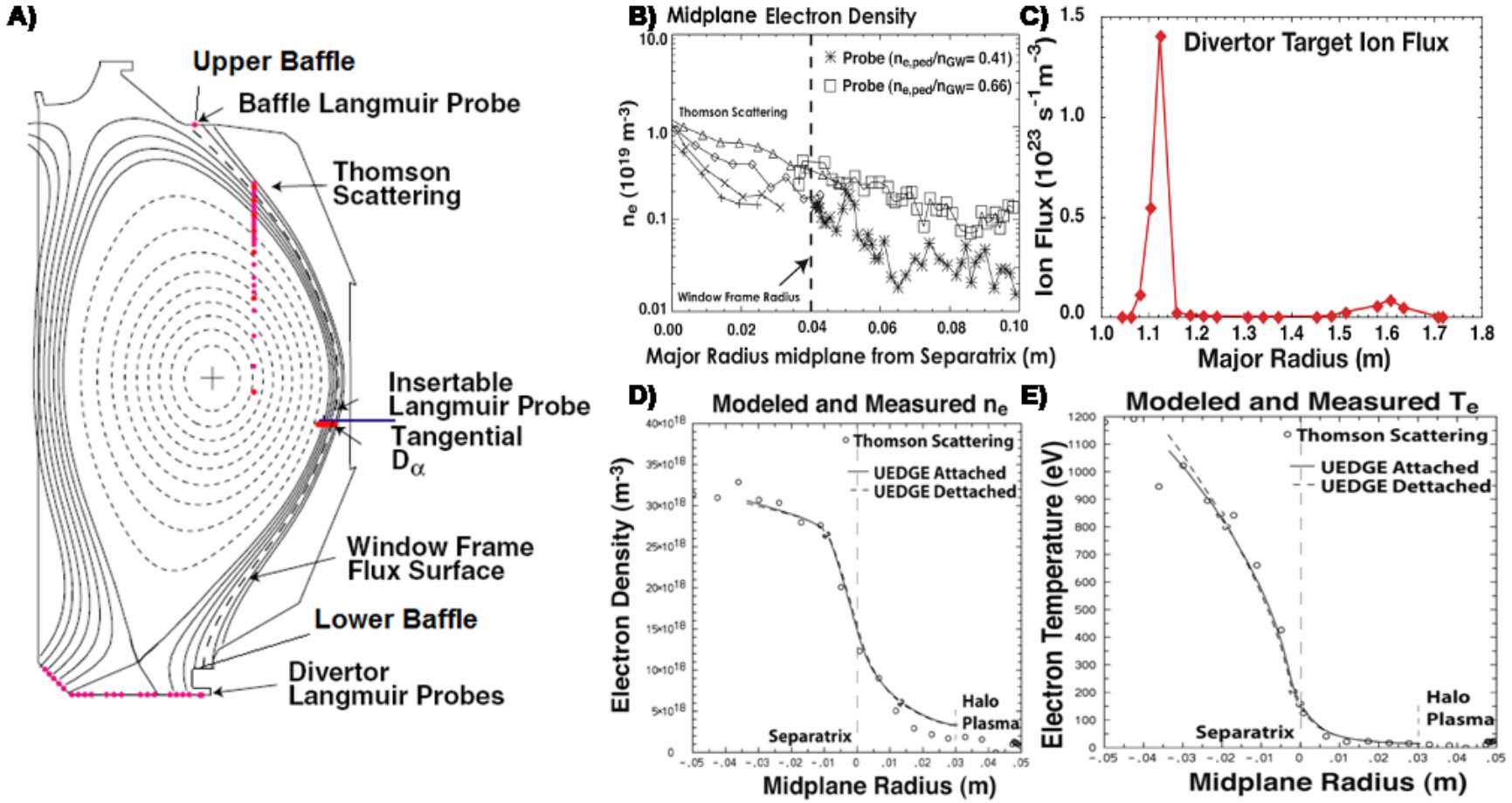
A)
Upper Baffle
Baffle Langmuir Probe
Thomson Scattering
Insertable Langmuir Probe
Tangential D_α
Window Frame Flux Surface
Lower Baffle
Divertor Langmuir Probes
B) Midplane Electron Density
Probe ($n_{e,ped}/n_{GW}$= 0.41)
Probe ($n_{e,ped}/n_{GW}$= 0.66)
Thomson Scattering
Window Frame Radius
n_e (10^{19} m^{-3})
Major Radius midplane from Separatrix (m)
C) Divertor Target Ion Flux
Ion Flux (10^{23} $s^{-1}m^{-3}$)
Major Radius (m)
D) Modeled and Measured n_e
Thomson Scattering
UEDGE Attached
UEDGE Dettached
Separatrix
Halo Plasma
Electron Density (m^{-3})
Midplane Radius (m)
E) Modeled and Measured T_e
Thomson Scattering
UEDGE Attached
UEDGE Dettached
Separatrix
Halo Plasma
Electron Temperature (eV)
Midplane Radius (m)

Ion Recycling & Recombination Sources (#/s)

From exp.

UPPER BAFFLE 8.13E+20
LOWER BAFFLE 8.13E+20
INNER DIVERTOR 5.55E+21
OUTER DIVERTOR 6.04E+21

From UEDGE

RECOMBINATION (attached) 0.147E+21
RECOMBINATION (detached) 6.243E+21

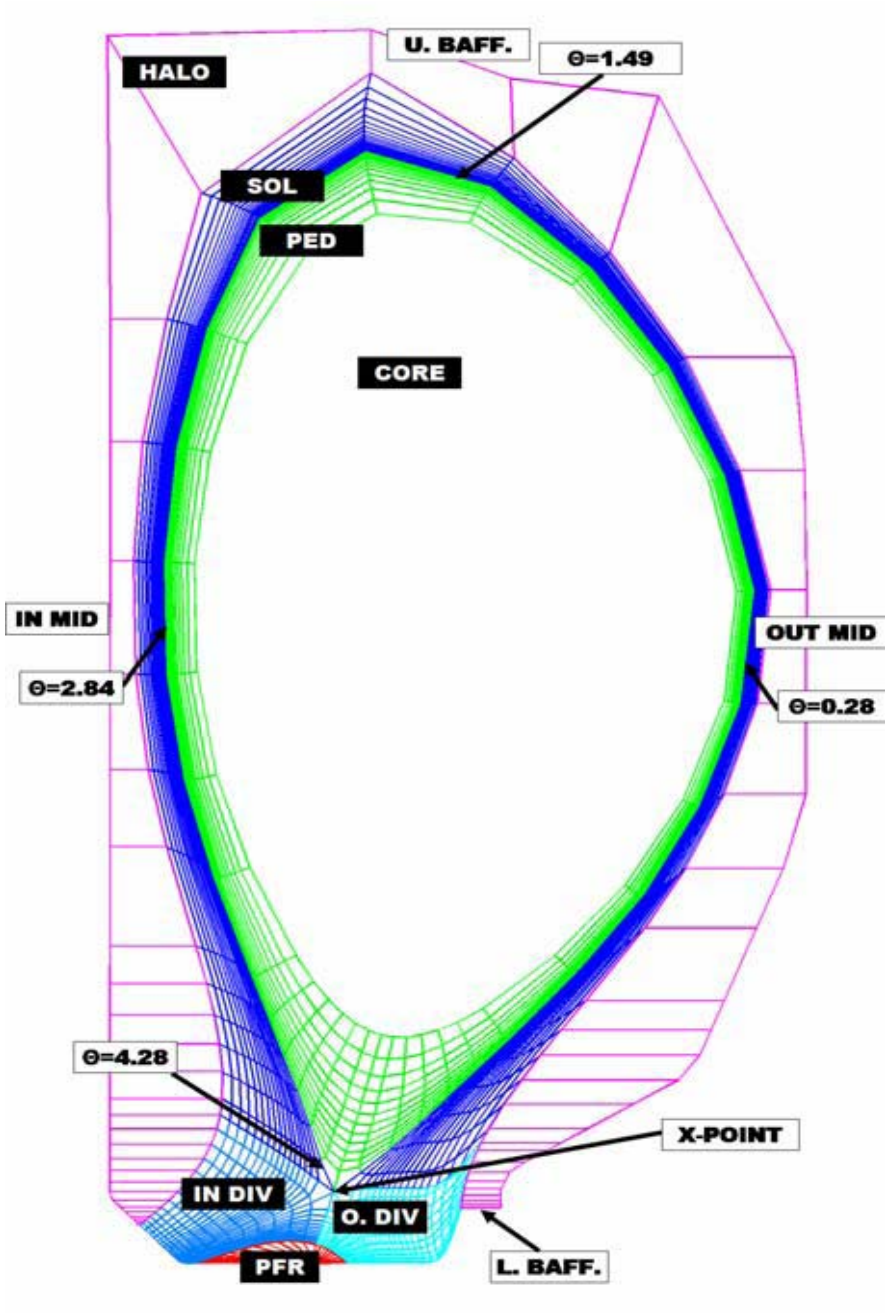
HALO
U. BAFF.
Θ=1.49
SOL
PED
CORE
IN MID
Θ=2.84
OUT MID
Θ=0.28
Θ=4.28
X-POINT
IN DIV
O. DIV
PFR
L. BAFF.

Neutral Particle Mean Free Path

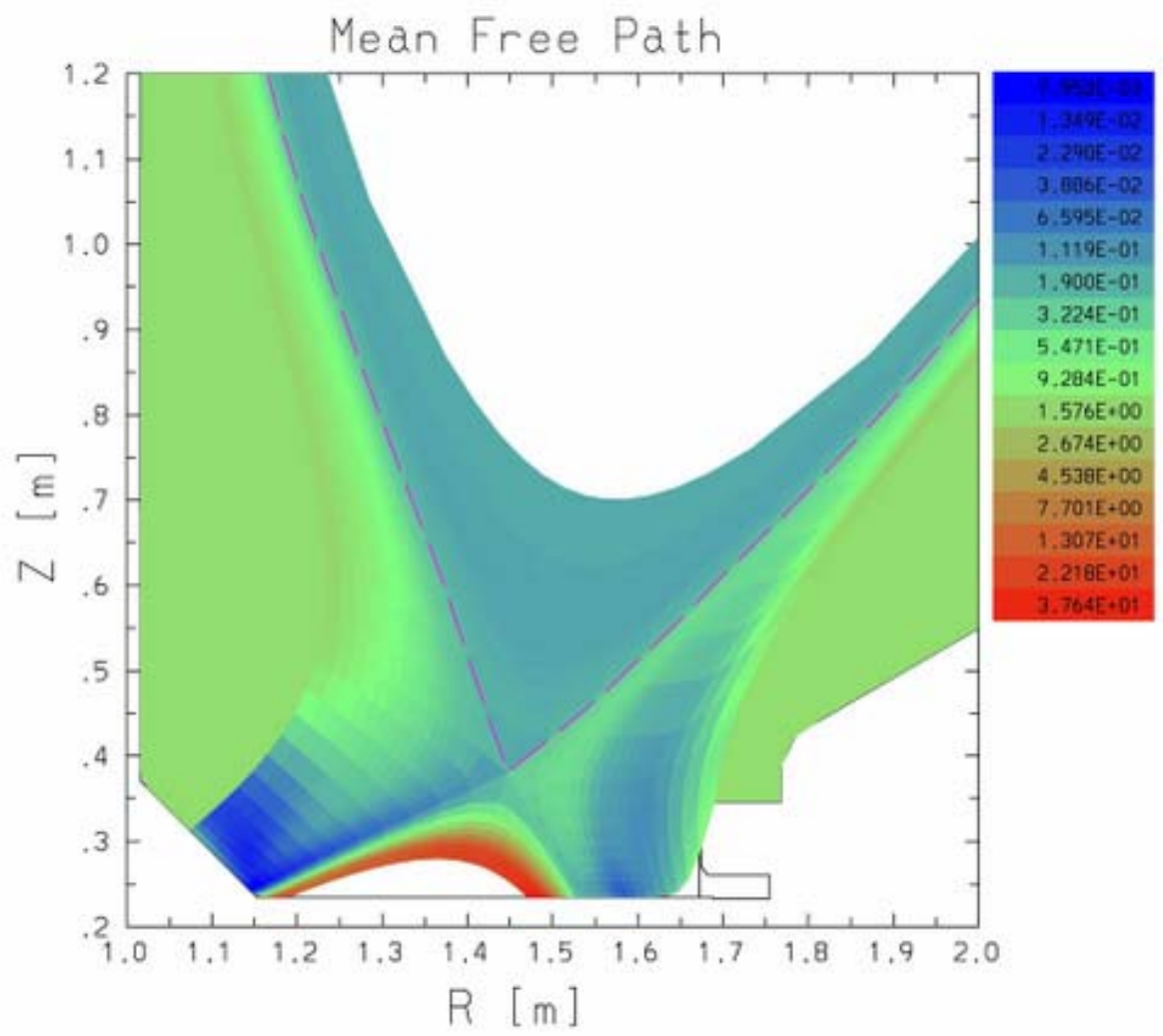

Poloidal Distribution—Neutral Fluxes Recycling from Wall

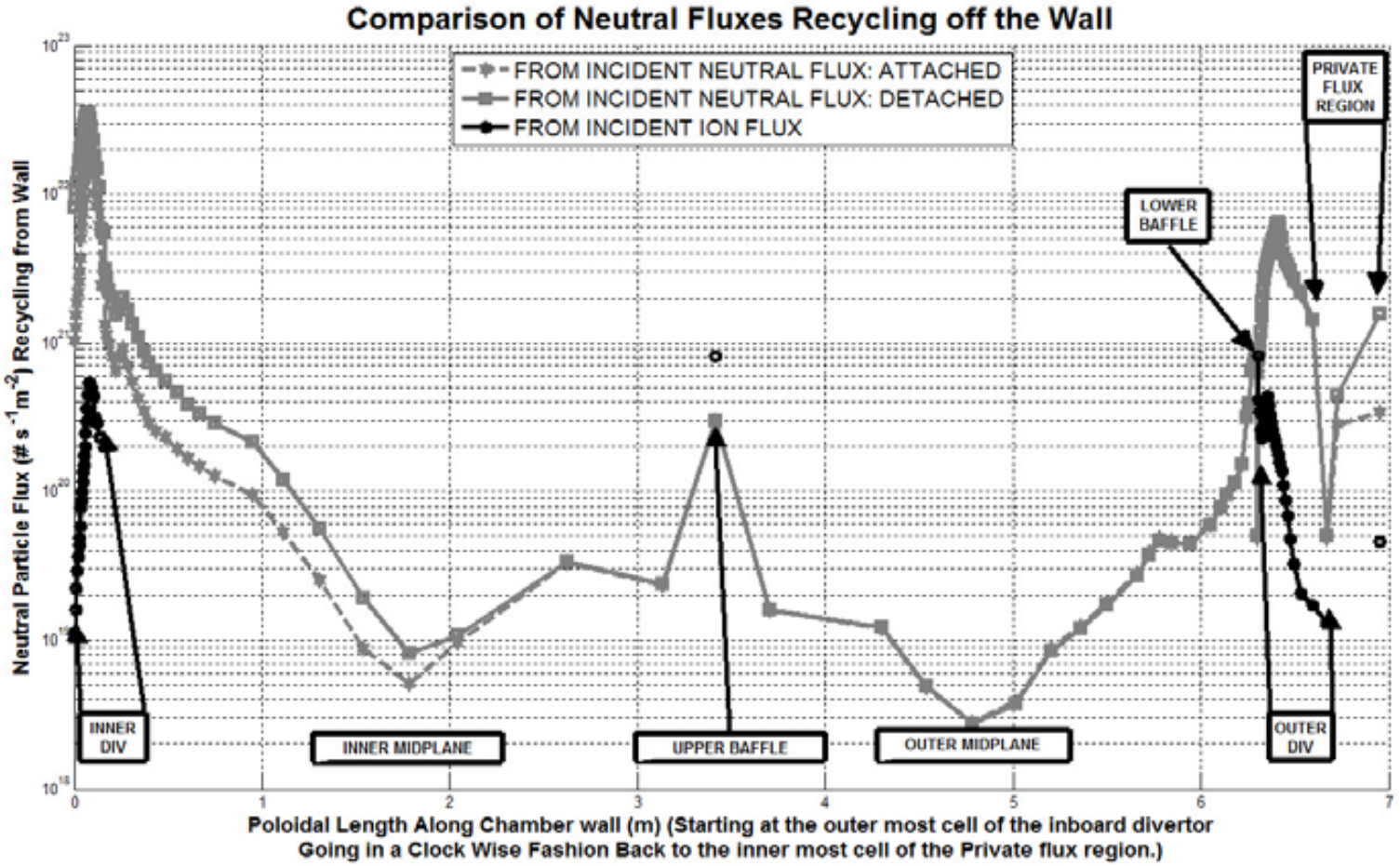

GTNEUT Inward Neutral Fluxes Across Separatrix

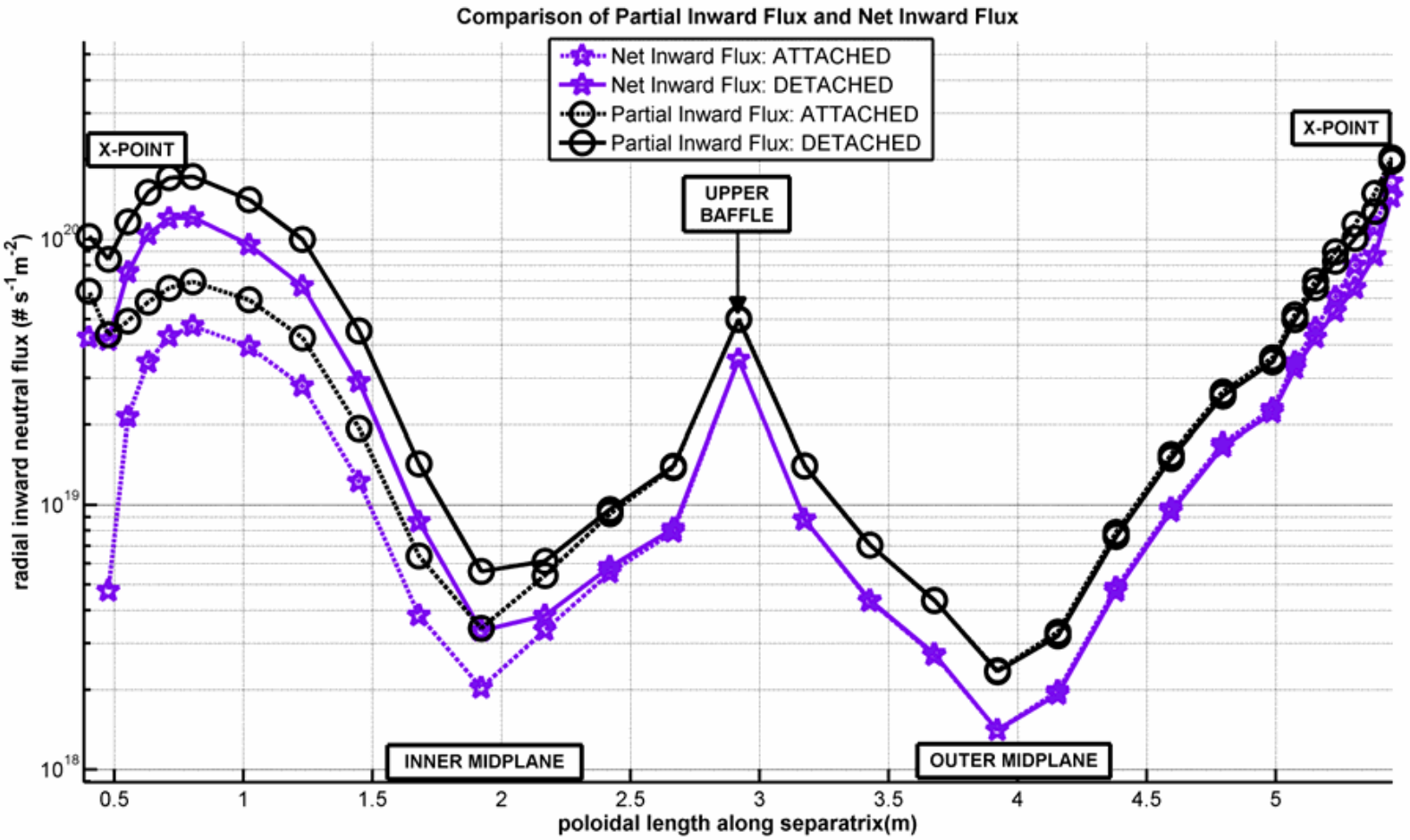

Global Neutral Particle Balance on Entire Computation Domain

	'Attached'	**'Detached'**	**Determined**
Ionization (Sinks) (#/s)			
CORE	0.129E+21 (1%)	0.193E+21 (1%)	GTNEUT
PED	0.798E+21 (6%)	1.120E+21 (6%)	"
SOL	1.910E+21 (15%)	2.670E+21 (14%)	"
HALO	1.120E+21 (9%)	2.020E+21 (11%)	"
IN DIV	4.380E+21 (33%)	7.390E+21 (39%)	"
OUT DIV	4.770E+21 (36%)	5.430E+21 (29%)	"
PFR	0.107E+19 (<<1%)	0.365E+19 (<<1%)	"
Total Ionization	**13.108E+21**	**18.827E+21**	
Sources (#/s)			
Ion recycling	13.217E+21 (99%)	13.217E+21 (66%)	experiment
Recombination	0.147E+21 (1%)	6.243E+21 (34%)	UEDGE
Total Sources	**13.364E+21**	**19.460E+21**	

Poloidal Distribution of Ionization Rates

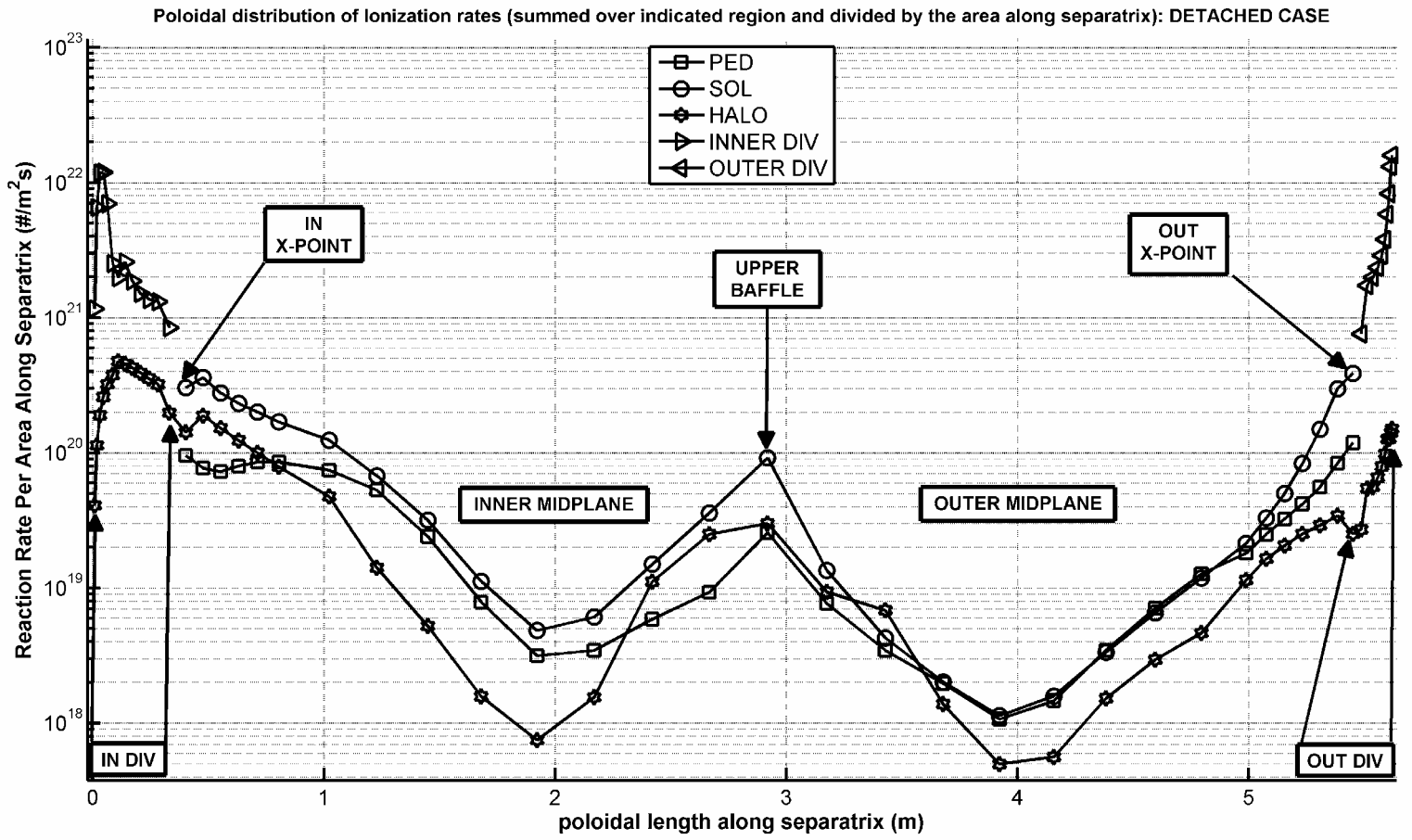

Poloidal Distribution of Charge-Exchange Rates

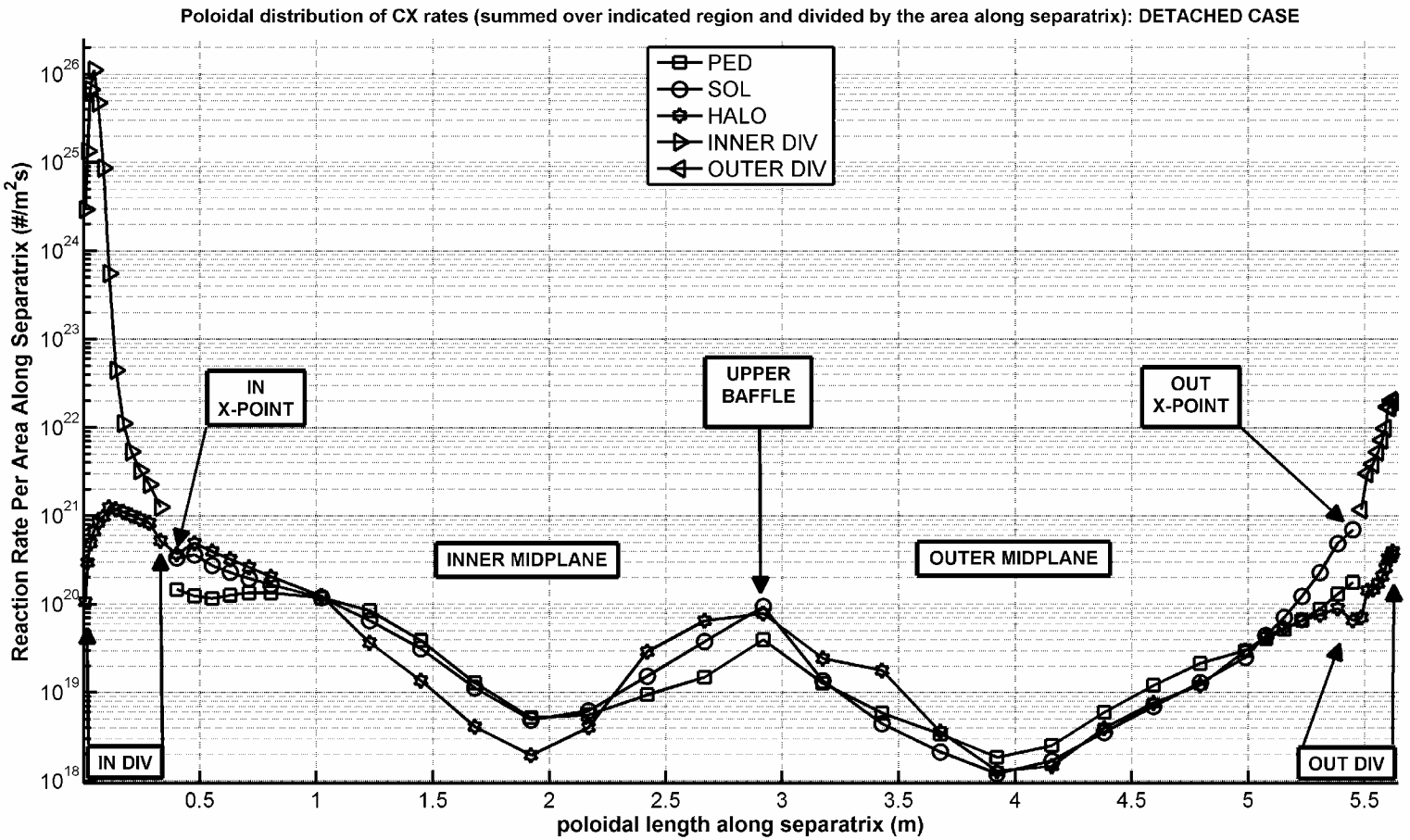

Poloidal Distribution of Neutral Density on Pedestal Flux Surfaces

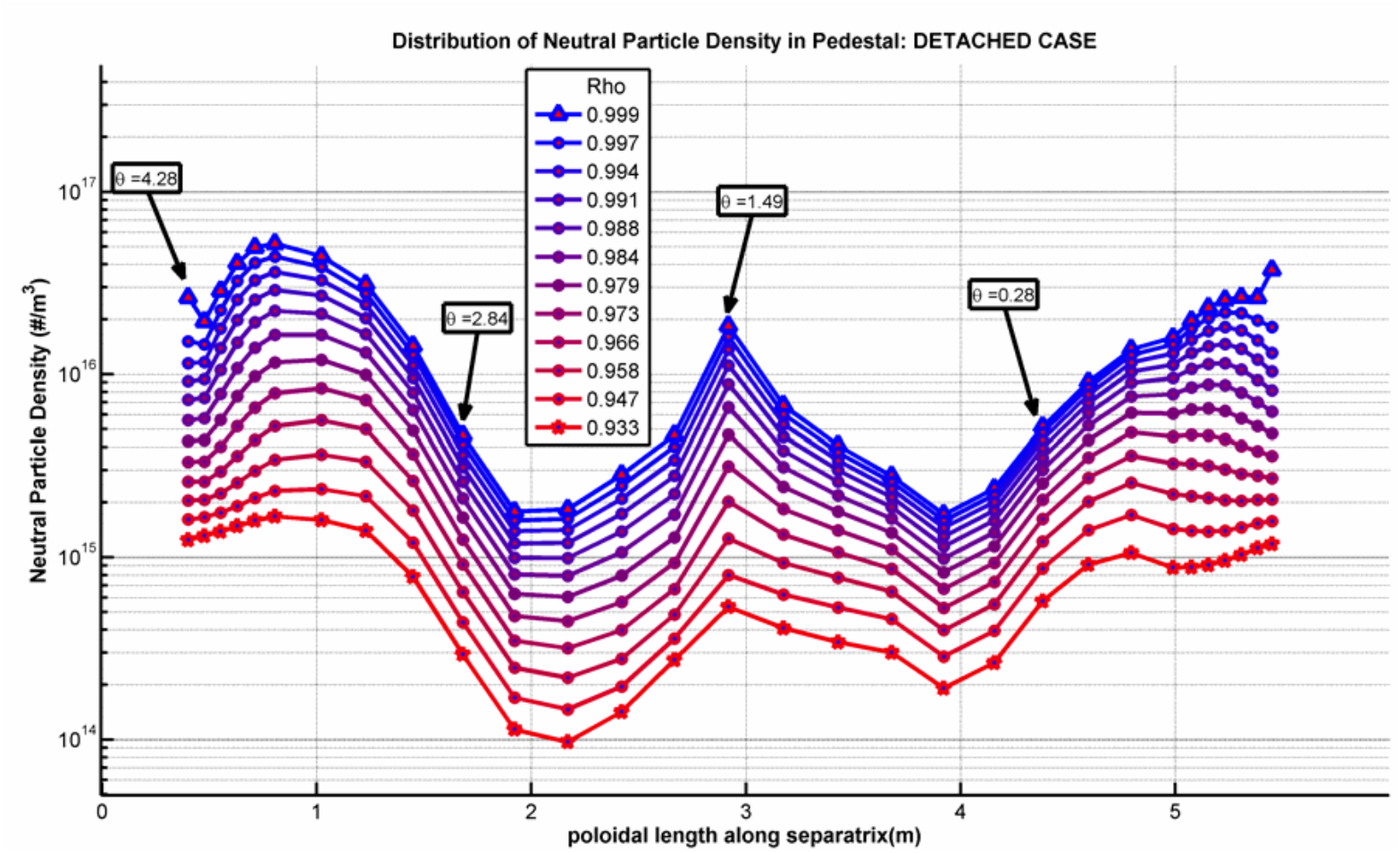

Poloidal Distribution of Ionization Rate on Pedestal Flux Surfaces

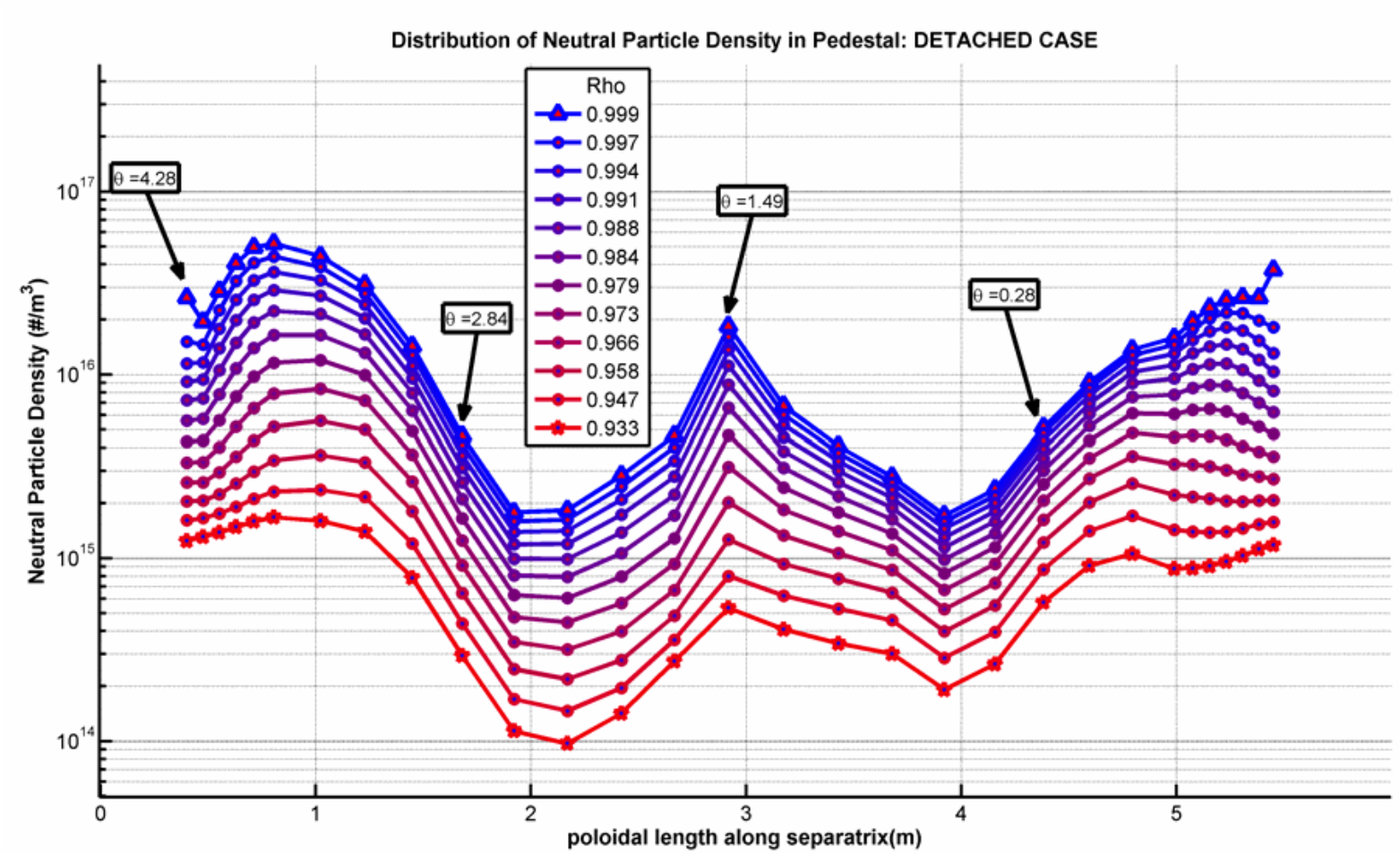

IMPLICATIONS

Order of magnitude variation of neutral density, ionization and charge-exchange rates on pedestal flux surface implies:

- A 2D, rather than a 1D, ion transport calculation is needed in the pedestal?
- If neutral penetration determines pedestal structure, then pedestal structure should display similar poloidal variation—exp?

Effectiveness of Individual Neutral Sources in Fueling Pedestal

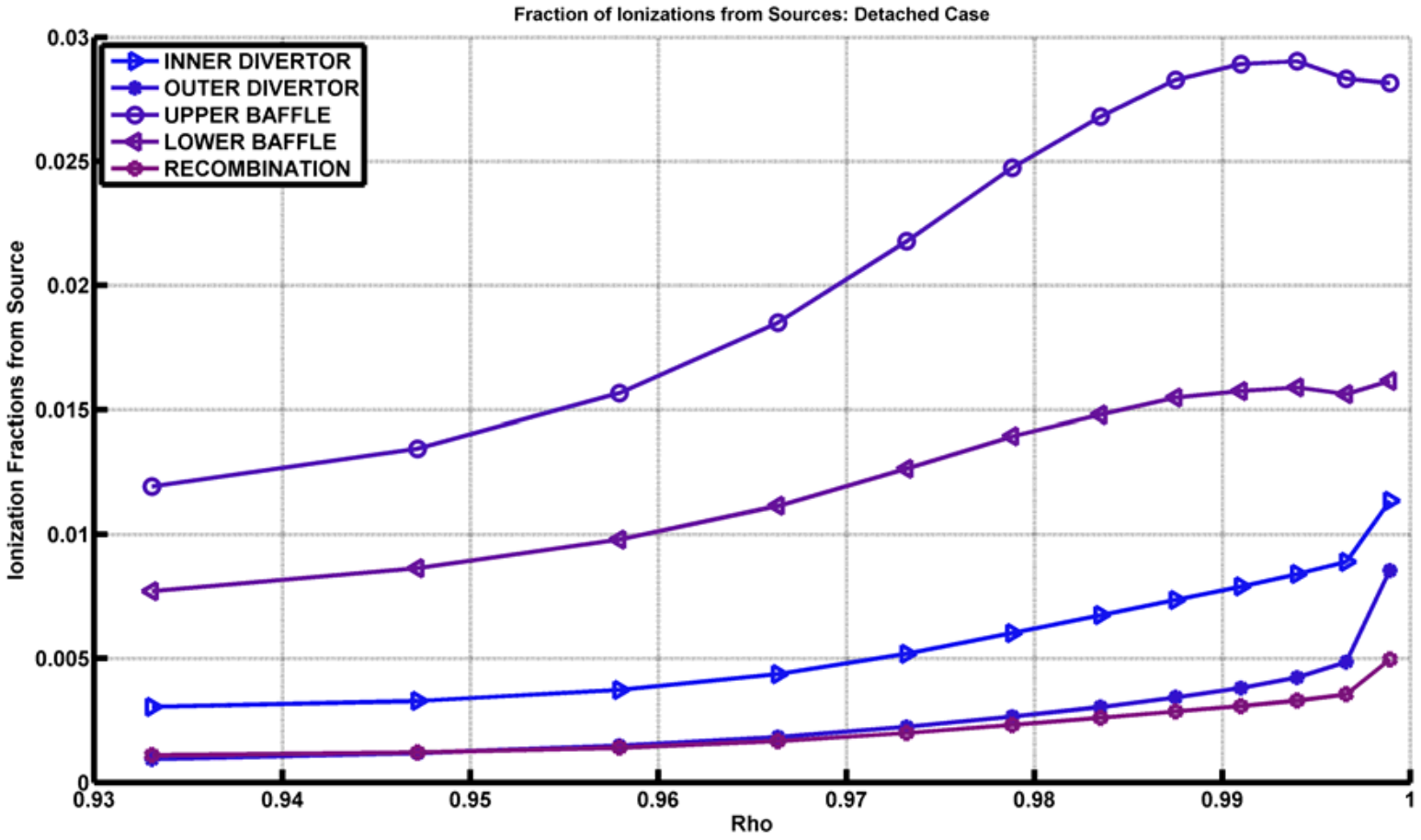

Ionization Rates in Pedestal from Individual Neutral Sources

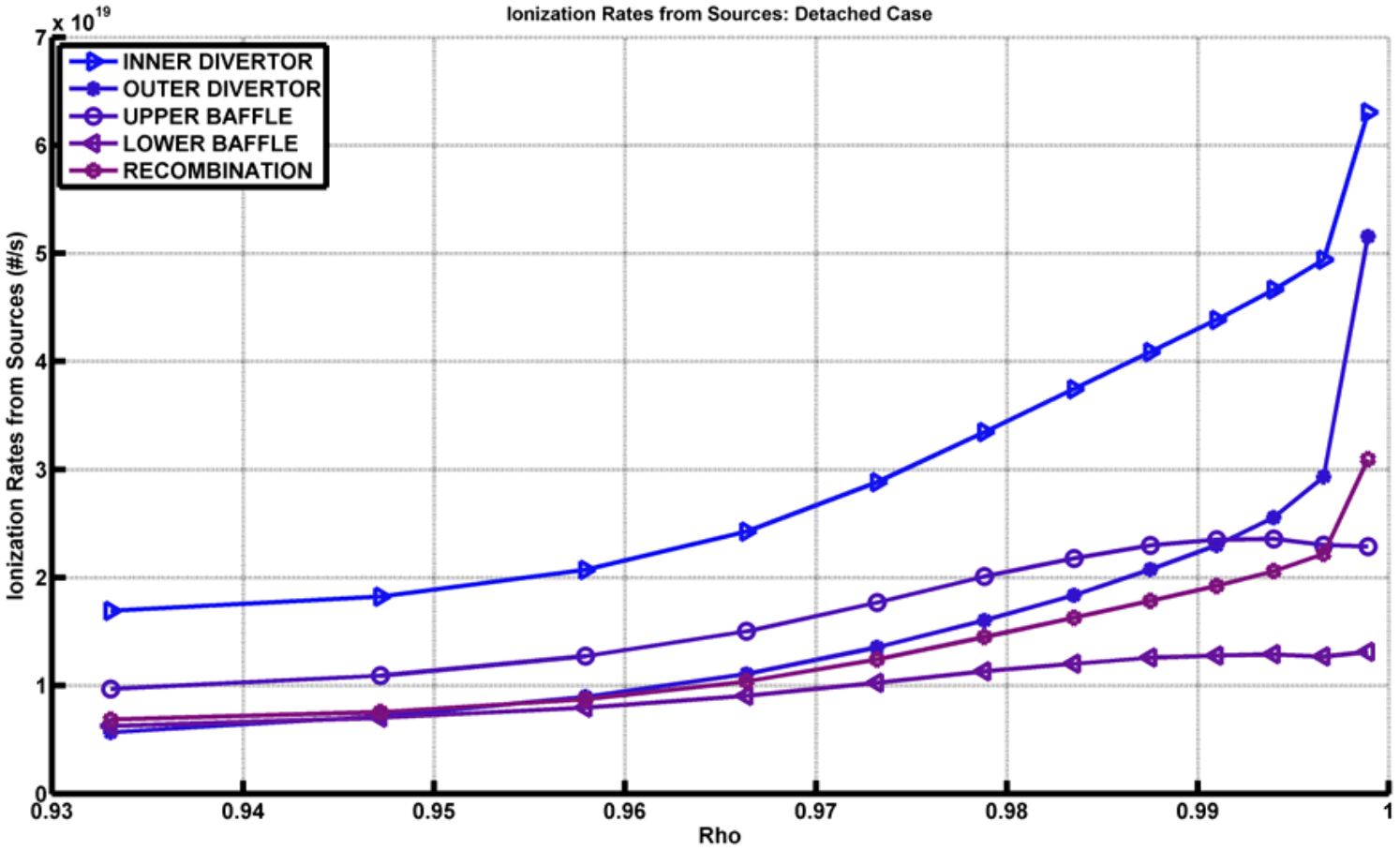

Fraction of neutrals from each source ionized in PED+CORE

	Fraction					
SOURCE	**ATTACHED**			**DETACHED**		
	PED	**CORE**	**PED+CORE**	**PED**	**CORE**	**PED+CORE**
Upper baffle recycling	17.5%	4.0%	**21.50%**	27.6%	5.4%	**33.00%**
Lower baffle recycling	15.2%	3.7%	**18.90%**	15.8%	3.6%	**19.40%**
Inner divertor recycling	4.0%	0.7%	**4.70%**	7.6%	1.5%	**9.10%**
Outer divertor recycling	4.7%	0.4%	**5.10%**	3.8%	0.3%	**4.10%**
Recombination	2.4%	1.3%	**3.70%**	3.0%	0.5%	**3.50%**

CONCLUSIONS

- Majority of recycling neutrals are ionized in the divertor; only about 7% cross the separatrix.
- Neutrals penetration into pedestal is highly non-uniform poloidally—i) need for 2D transport calc. in PED?; ii) poloidally non-uniform pedestal structure if neutrals determine structure?
- Neutrals recycling from baffle are more effective in penetrating pedestal than neutrals recycling from divertor target, but
- Majority of pedestal fueling is due to neutrals recycling or recombining in divertor.

Access to GTNEUT & Documentation

- CODES

GTNEUT **u4/friis/GTNEUT/**

Geometry Input **/u4/friis/uedge/GTNEUT_DEMO**

- DOCUMENTATION

Methodology—Nucl. Fusion,34,1385(1994);
Phys. Plasmas 13, 062509(2006).

Code—Comp. Phys. 161,36(2004).

Automated Geometry & Background Plasma Input from UEDGE---User's Manual at www.frc.gatech.edu on "Neutrals" page.

Global Ion Particle Balance on CORE+PED

	'Attached'	'Detached'	Determined
Loss--Ion Outflow Across Separatrix (#/s)	**2.74E+21**	**2.74E+21**	Experiment
Sources			
Neutral Beam Ion Source(#/s)	0.386E+21	0.386E+21	Known
Ionization of Recycling Neutrals (#/s)	0.927E+21	1.313E+21	GTNEUT
Total Ion Source(#/s)	**1.316E+21**	**1.699E+21**	
Ion (Outflow – Sources) (#/s)	**1.424E+21 (108%)**	**1.041E+21 (61%)**	

Comparison of GTNEUT & DEGAS2 Calculation of Pedestal Ionization Rates—'Attached'

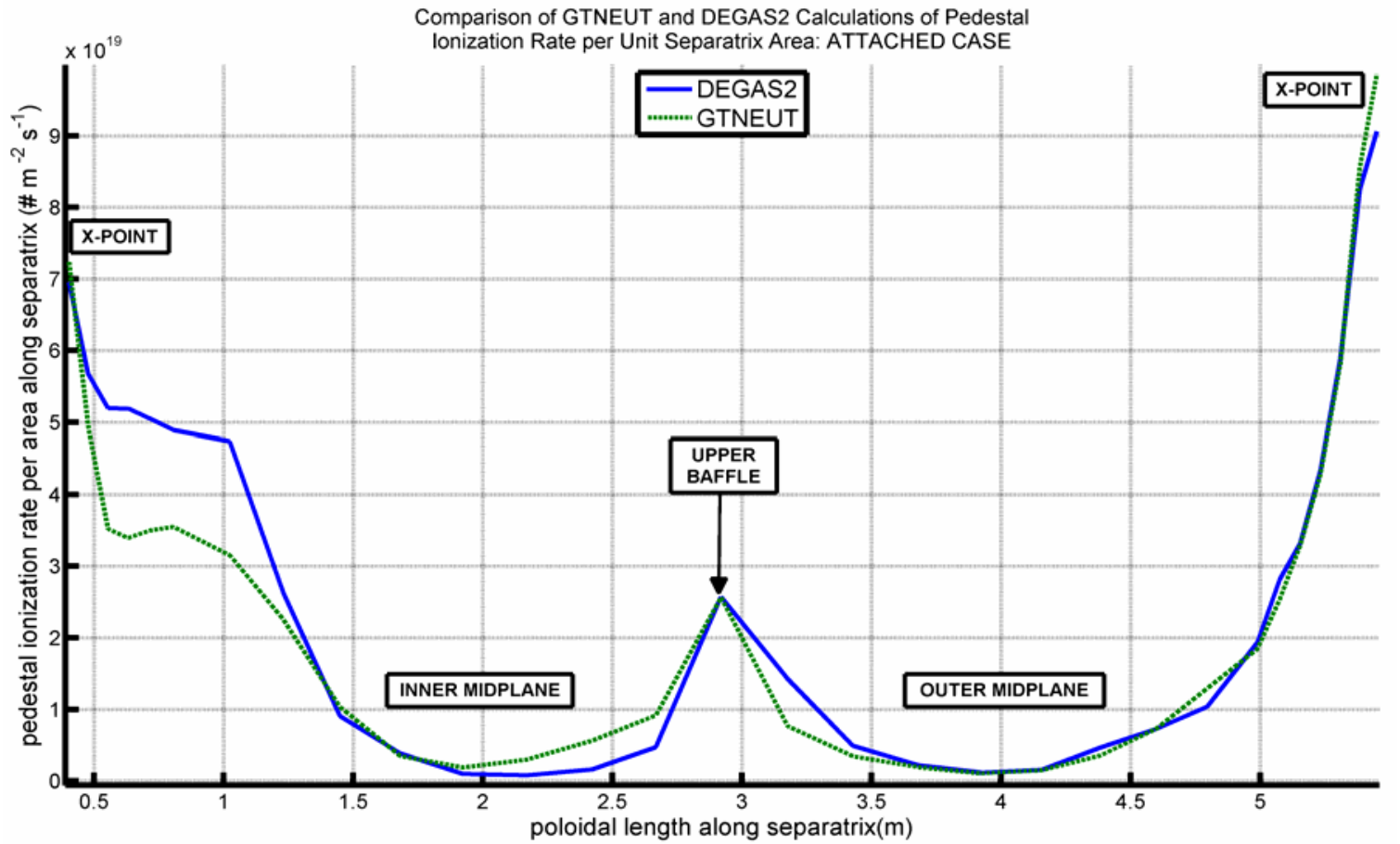

Comparison of GTNEUT & DEGAS2 Calculation of Pedestal Ionization Rates—'Detached'

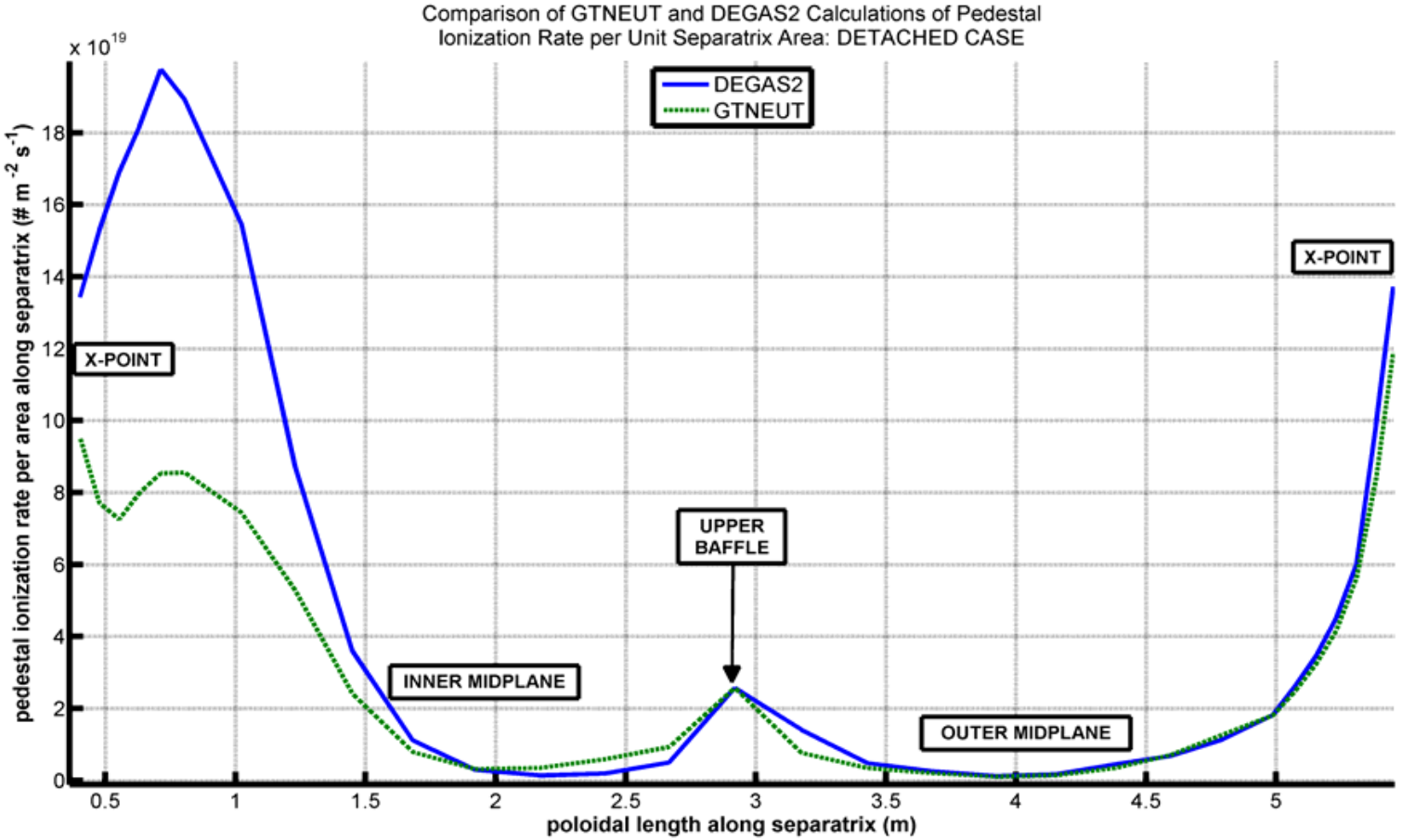

Comparison of ionization rates in the PED+CORE calculated by GTNEUT and DEGAS2

	GTNEUT		DEGAS2	
	'Attached'	**'Detached'**	**'Attached'**	**'Detached'**
Source Strength (#/s)	1.34E+22	1.96E+22	1.34E+22	1.96E+22
Ionization Rate (#/s) PED + CORE	0.927E+21	1.313E+21	0.860E+21	1.77E+21
Percent of Source Neutrals Ionized in PED + CORE	6.9%	6.7%	6.4%	9.0%
Calculation Uncertainty	1.8%	3.2%	5%	5%

Particle Pinch and Diffusion Coefficients in the Edge Pedestal

W. M. Stacey, Georgia Tech
R. J. Groebner, General Atomics

November, 2009

We develop a formalism to infer particle pinches and diffusion coefficients from experimental data and apply it to two DIII-D shots.

Derivation

The toroidal and radial components of the momentum balance for ion species "j" can be written as

$$n_j m_j \left[\left(\nu_{jk} + \nu_{dj} \right) V_{\phi j} - \nu_{jk} V_{\phi k} \right] = n_j e_j E_\phi^A + n_j e_j B_\theta V_{rj} + M_{\phi j} \quad (1)$$

and

$$V_{\phi j} = \frac{1}{B_\theta} \left[E_r + V_{\theta j} B_\phi - \frac{1}{n_j e_j} \frac{\partial p_j}{\partial r} \right] \quad (2)$$

Using Eq. (2) to eliminate the toroidal velocities for both species, Eq. (1) may be rewritten

$$V_{rj} = -\frac{m_j \left(\nu_{jk} + \nu_{dj} \right) T_j}{\left(e_j B_\theta \right)^2} \left[\left(\frac{1}{p_j} \frac{\partial p_j}{\partial r} \right) - \frac{e_j}{e_k} \frac{\nu_{jk}}{\left(\nu_{jk} + \nu_{dj} \right)} \left(\frac{1}{p_k} \frac{\partial p_k}{\partial r} \right) \right] + V_{rj}^{pinch} \quad (3)$$

where

$$V_{rj}^{pinch} = \frac{1}{e_j B_\theta} \left[-\left(e_j E_\phi^A + \frac{M_{\phi j}}{n_j} \right) + \frac{m_j \nu_{dj}}{B_\theta} \left(E_r + V_{\theta j} B_\phi \right) + \frac{m_j \nu_{jk} B_\phi}{B_\theta} \left(V_{\theta j} - V_{\theta k} \right) \right] \quad (4)$$

Derivation (continued 2)

This equation can be simplified to the form

$$V_{rj} \simeq -D_j \left(\frac{1}{p_j} \frac{\partial p_j}{\partial r} \right) + V_{rj}^{pinch} \qquad (5)$$

Eq. (5) can be used to infer the experimental particle diffusion coefficient

$$D_j^{\exp} = \left(V_{rj} - V_{rj}^{pinch} \right) \frac{L_{nj}^{\exp} L_{Tj}^{\exp}}{\left(L_{nj}^{\exp} + L_{Tj}^{\exp} \right)} \qquad (6)$$

once V_{rj}^{pinch} and ν_{dj} are determined

Determination of Momentum Transfer Frequency

Solving Eqs. (1) for the momentum transfer frequencies for the two plasma species, j and k, using a perturbation analysis in the assumed small parameter $\left(1 - V_{\phi j}/V_{\phi k}\right)$, yields to leading order

$$\nu_{dj} = \frac{(n_j e_j E_\phi^A + n_j e_j B_\theta V_{rj} + M_{\phi j}) + (n_k e_k E_\phi^A + n_k e_k B_\theta V_{rk} + M_{\phi k})}{\left(n_j m_j + n_k m_k\right) V_{\phi k}^{\exp}} \qquad \text{(A.1)}$$

and

$$\left(V_{\phi j} - V_{\phi k}\right)_0 = \frac{\left(n_j e_j E_\phi^A + n_j e_j B_\theta V_{rj} + M_{\phi j}\right) - n_j m_j \nu_{dj} V_{\phi k}^{\exp}}{n_j m_j \left(\nu_{jk} + \nu_{dj}\right)} \qquad \text{(A.2)}$$

and to first order

$$\nu_{dk} = \frac{(n_k e_k E_\phi^A + n_k e_k B_\theta V_{rk} + M_{\phi k}) + n_k m_k \nu_{kj} \left(V_{\phi j} - V_{\phi k}\right)_0}{n_k m_k V_{\phi k}^{\exp}} \qquad \text{(A.3)}$$

Experimental Data for Shot 98889

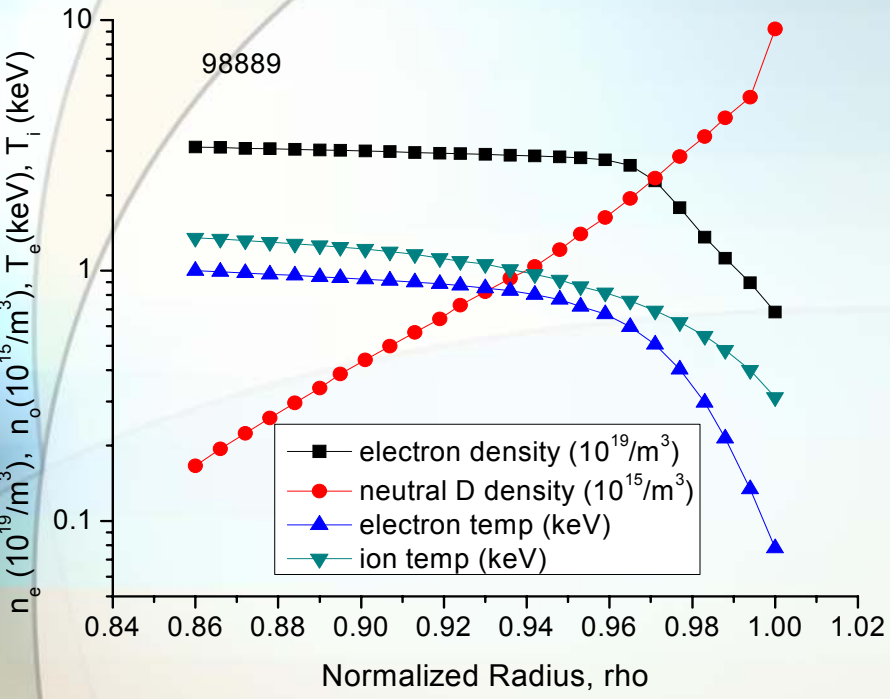

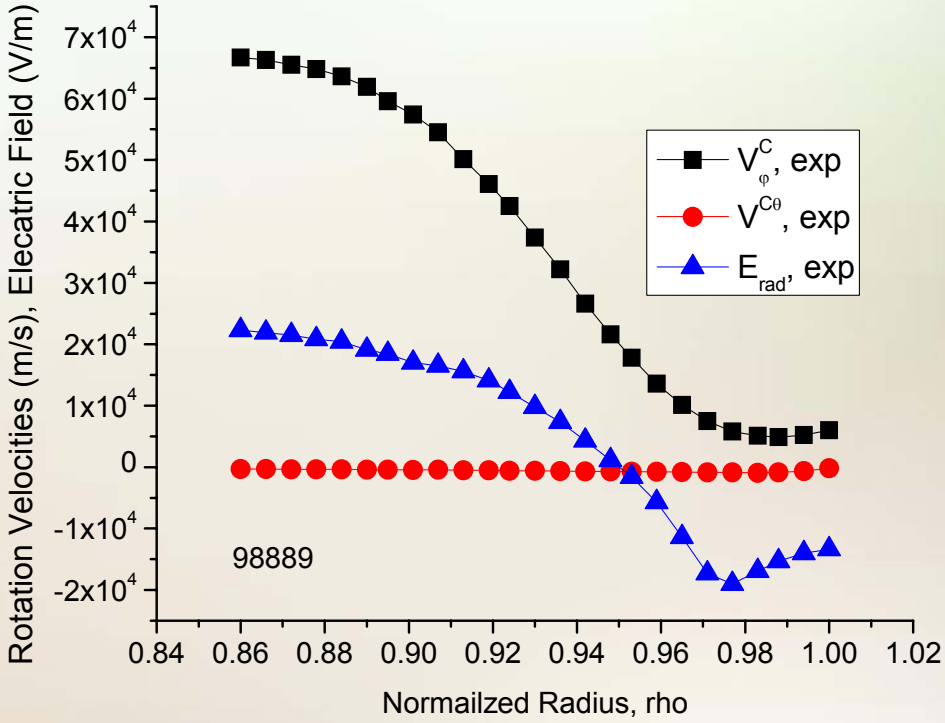

Infered Momentum Transfer Frequencies and Pinch Velocity for 98889

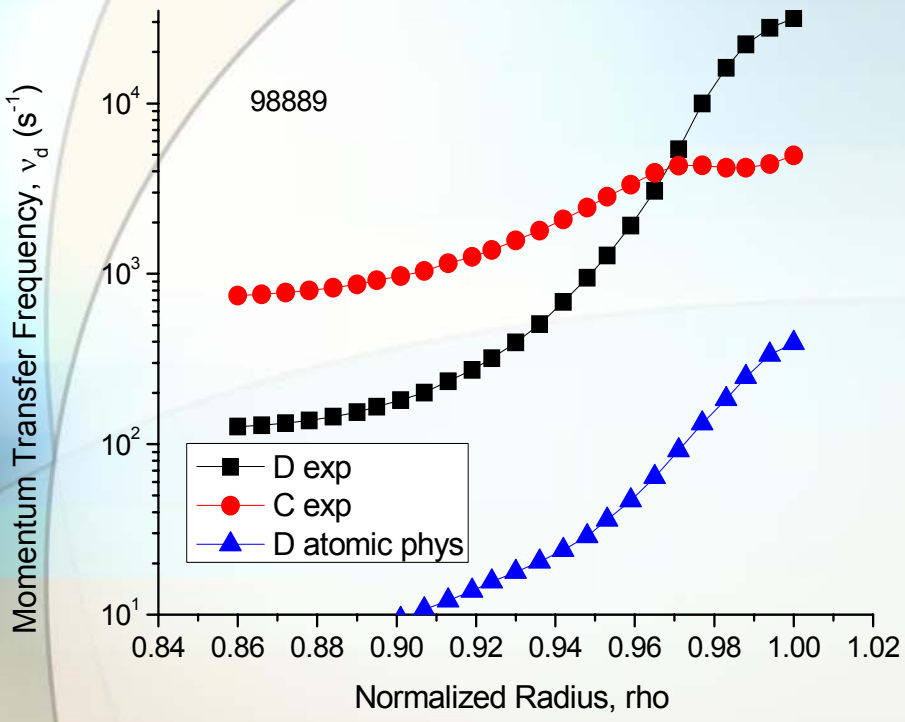

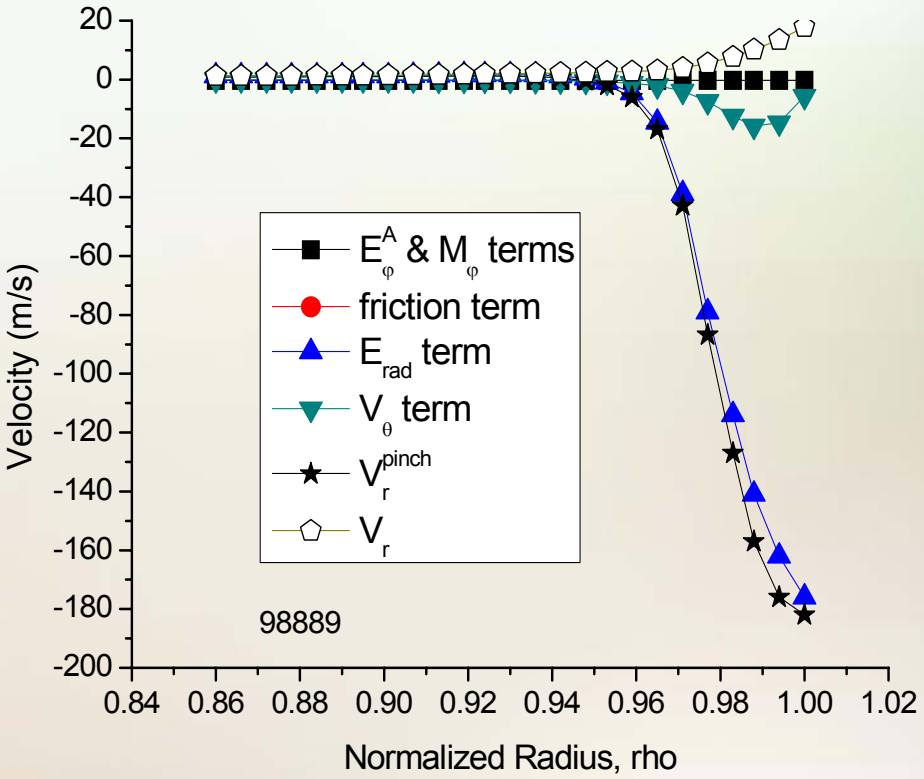

Deuterium Diffusion Coefficient for 98889

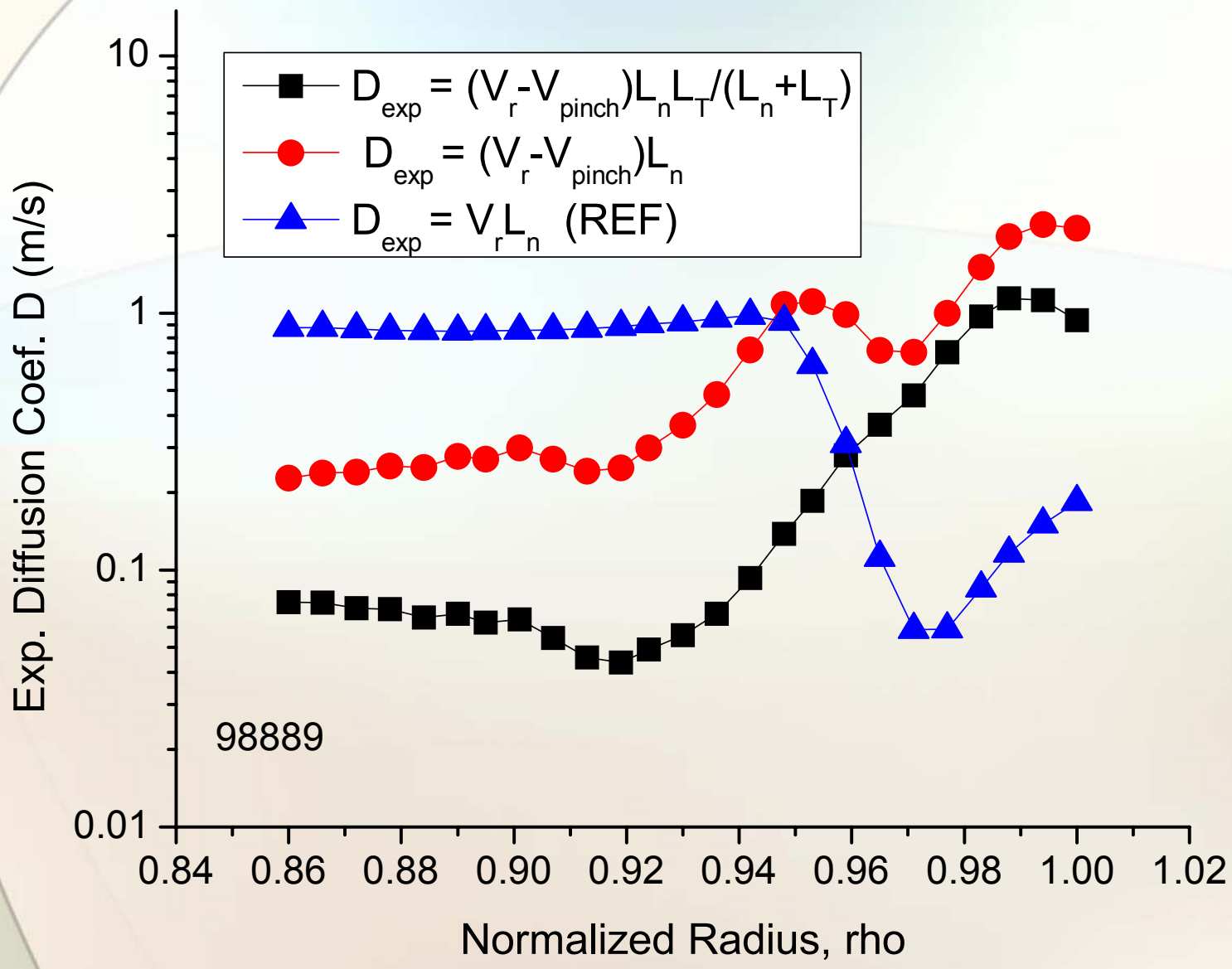

Experimental Data for 119436

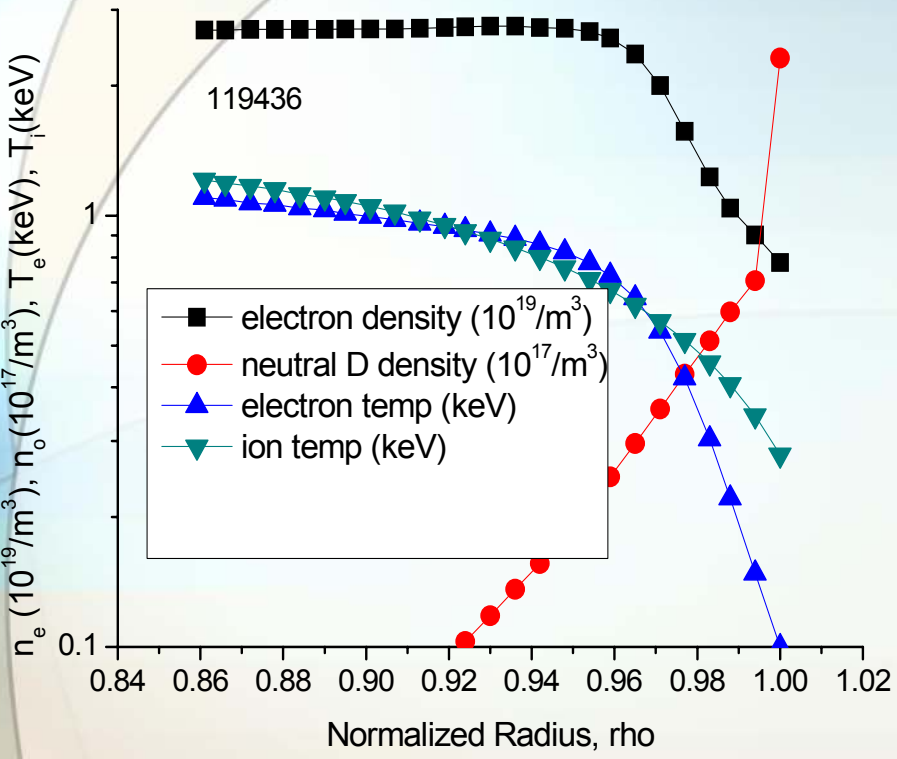

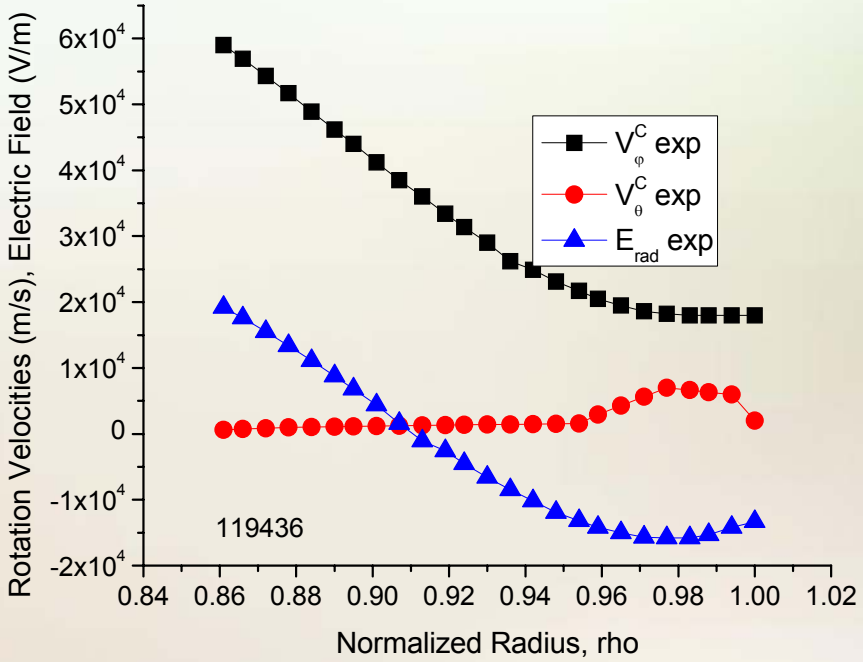

Pinch Velocity for 119436

Alternative form

$$V_{rj}^{pinch} = \frac{1}{e_j B_\theta}\left[-\left(e_j E_\phi^A + \frac{M_{\phi j}}{n_j}\right) + \frac{m_j\left(\nu_{jk}+\nu_{dj}\right)}{B_\theta}\left(E_r + V_{\theta j} B_\phi\right) - m_j \nu_{jk} V_{\phi k}\right] \qquad (7)$$

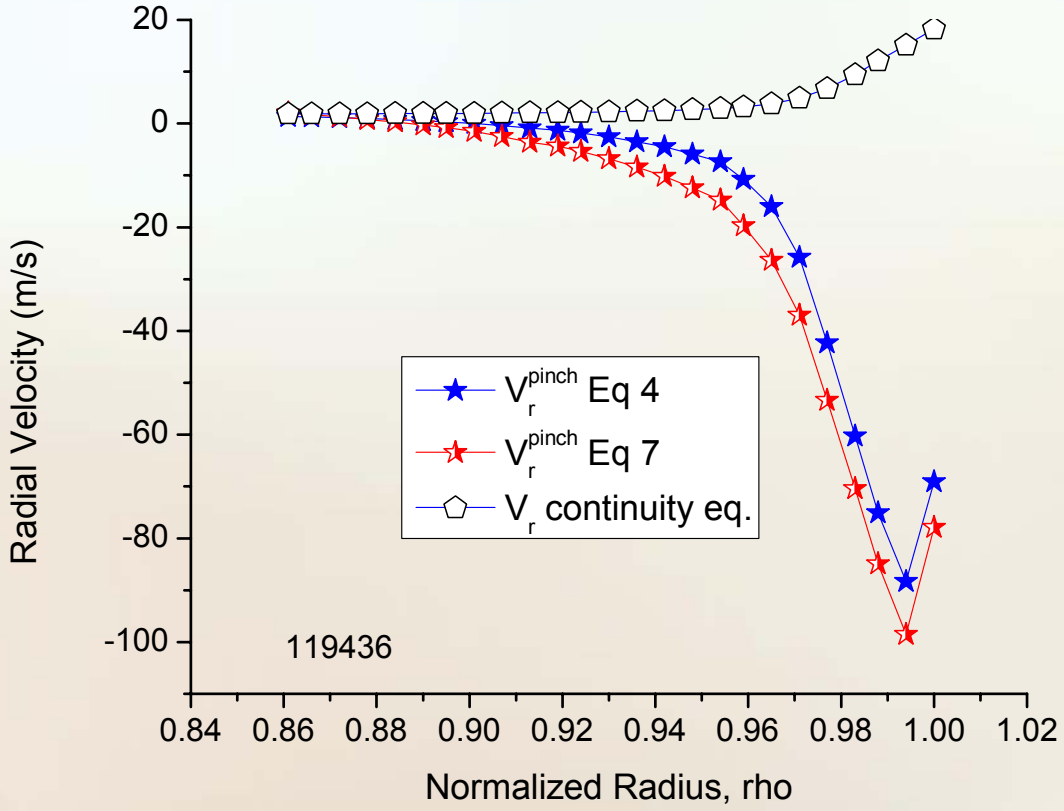

Diffusion Coefficient for 119436

When Eq. (2) was used in Eq. (1) to obtain Eqs. (4) and (5), an explicit expression was also obtained for the diffusion coefficient in Eq. (5)

$$D_j^{\exp} = \frac{m_j \left(\nu_{jk} + \nu_{dj}\right) T_j}{\left(e_j B_\theta\right)^2} \qquad (8)$$

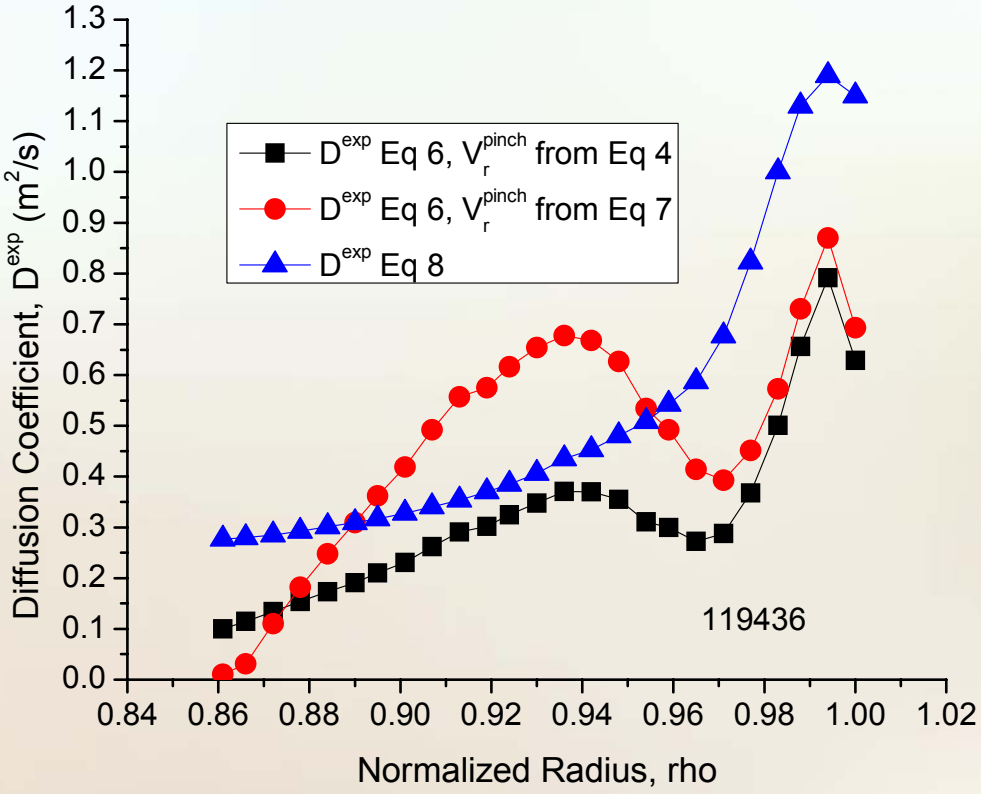

CONCLUSIONS

- There is a large inward particle pinch in the edge pedestal which can be evaluated from experimental data.
- When this particle pinch is taken into account in interpreting the experimental particle diffusion coefficient, D^{exp} increases rather than decreases in the edge pedestal.
- Thus, it seems that the 'particle transport barrier' inferred from previous interpretations of diffusion coefficients using purely diffusive models were an artifact of neglecting the large inward pinch.

GENERALIZED DIFFUSION THEORY CALCULATIONS OF THE EDGE PEDESTAL DENSITY PROFILE

J-P. Floyd and W. M. Stacey
Georgia Tech
November, 2009

Overview

- A generalized diffusion theory has been derived based on a pinch-diffusion relation for the ion particle flux[1]
- A methodology for interpreting the pinch velocity and the diffusion coefficient from experimental data has been developed[2]
- This work examines the numerical solution of the generalized diffusion equation using the D and Vpinch inferred from experiment

Pinch-Diffusion Relation

- The toroidal and radial momentum balances

$$n_j m_j \left[\left(\nu_{jk} + \nu_{dj} \right) V_{\phi j} - \nu_{jk} V_{\phi k} \right] = n_j e_j E_\phi^A + n_j e_j B_\theta V_{rj} + M_{\phi j} \quad (1)$$

$$V_{\phi j} = \frac{1}{B_\theta} \left[E_r + V_{\theta j} B_\phi - \frac{1}{n_j e_j} \frac{\partial p_j}{\partial r} \right] \quad (2)$$

- Lead[1] to a pinch-diffusion relation

$$V_{rj} = -\frac{m_j \left(\nu_{jk} + \nu_{dj} \right) T_j}{\left(e_j B_\theta \right)^2} \left[\left(\frac{1}{p_j} \frac{\partial p_j}{\partial r} \right) - \frac{e_j}{e_k} \frac{\nu_{jk}}{\left(\nu_{jk} + \nu_{dj} \right)} \left(\frac{1}{p_k} \frac{\partial p_k}{\partial r} \right) \right] + V_{rj}^{pinch} \quad (3)$$

$$V_{rj}^{pinch} = \frac{1}{e_j B_\theta} \left[-\left(e_j E_\phi^A + \frac{M_{\phi j}}{n_j} \right) + \frac{m_j \nu_{dj}}{B_\theta} \left(E_r + \upsilon_{\theta j} B_\phi \right) + \frac{m_j \nu_{jk} B_\phi}{B_\theta} \left(\upsilon_{\theta j} - \upsilon_{\theta k} \right) \right] \quad (4)$$

Diffusion Equation

- Using (3) in the continuity equation

$$\nabla \cdot \Gamma_{rj} \equiv \nabla \cdot n_j v_j = S_j \qquad (5)$$

- yields a diffusion equation[1]

$$-\frac{\partial}{\partial r}\left(D_{jj} \frac{\partial n_j}{\partial r} \right) - \frac{\partial}{\partial r}\left(D_{jj} \left(\frac{n_j}{T_j} \right) \frac{\partial T_j}{\partial r} \right) + \frac{\partial}{\partial r}\left(n_j v_{pj} \right) = S_j \qquad (6)$$

Experimental Determination of Parameters

- The pinch velocity of (f) can be determined from experiment.
- Fitting measured density and temperature profiles produce[2]

$$D_j^{\exp} = \left(V_{rj} - V_{rj}^{pinch}\right) \frac{L_{nj}^{\exp} L_{Tj}^{\exp}}{\left(L_{nj}^{\exp} + L_{Tj}^{\exp}\right)} \qquad (7)$$

Numerical Solution

- Equation (6) is numerically integrated

$$a_{i,i-1}n_{i-1} + a_{i,i}n_i + a_{i,i+1}n_{i+1} = S_i \quad (8)$$

$$a_{i,i+1} = \frac{\alpha_{i+1} + \alpha_i}{2\Delta^2} \quad (9) \qquad a_{i,i} = \frac{2\Delta\beta_i - \alpha_{i+1} - 2\alpha_i - \alpha_{i-1}}{2\Delta^2} \quad (10)$$

$$a_{i,i-1} = \frac{\alpha_i + \alpha_{i-1} - 2\Delta\beta_{i-1}}{2\Delta^2} \quad (11) \qquad \alpha_i = -D_i \quad \beta_i = \frac{D_i}{L_T} + V_{ri}^{pinch} \quad (12)$$

- and solved via Gaussian elimination for the density

Experimental Data - shot 98889[2]

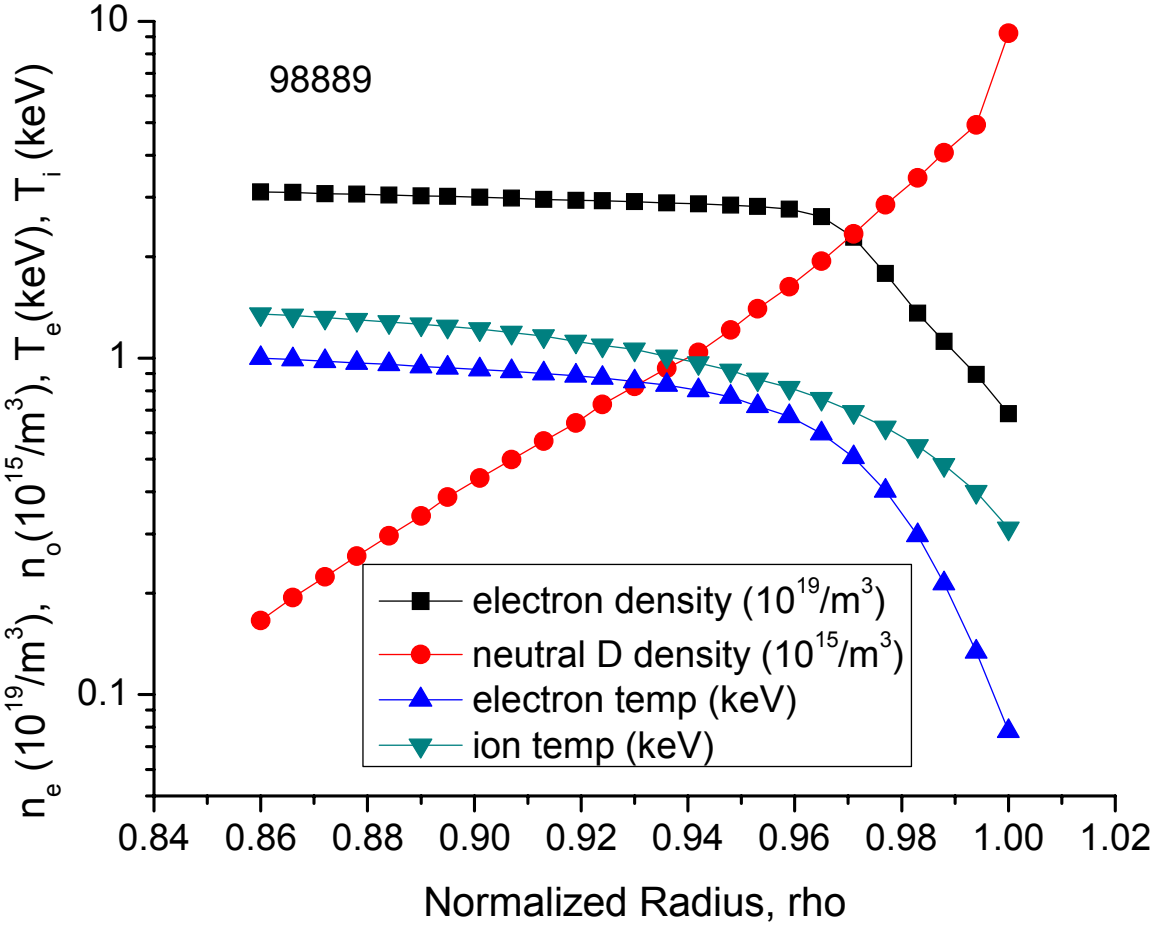

Calculated Density and Ion Diff. Coeff.

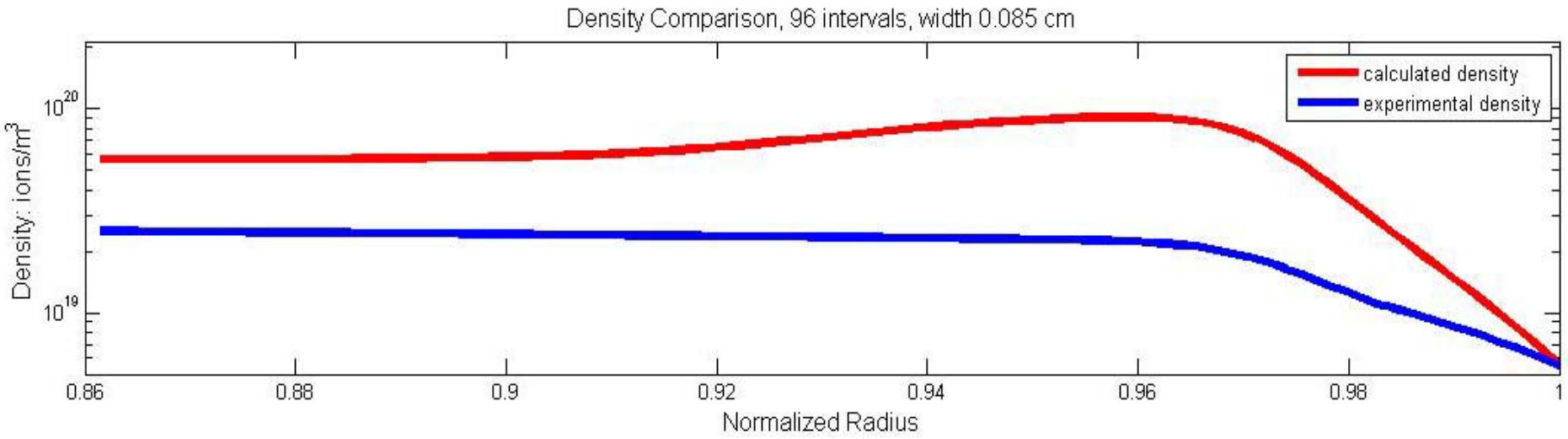

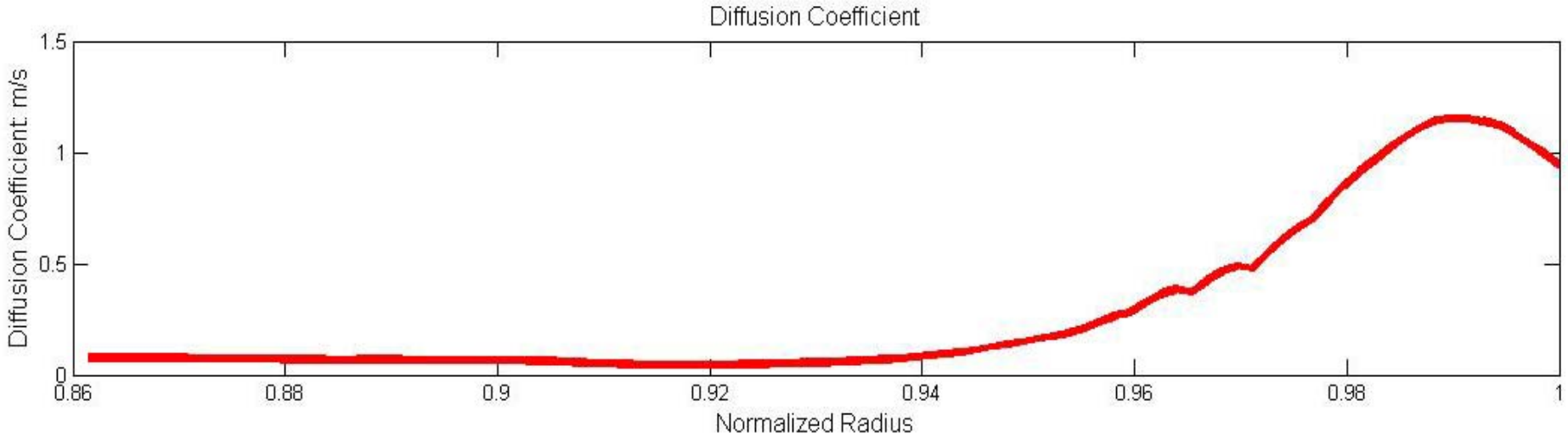

Interval Size Sensitivity

- For diffusion theory to be accurate, the interval width must be smaller than the mean free path.
- The expressio shown

$$\lambda_i \cong \sqrt{\frac{D_i}{\left(\nu_{iz} + \nu_{di}^*\right)}} \quad (13)$$

- The mean free path is plotted here.

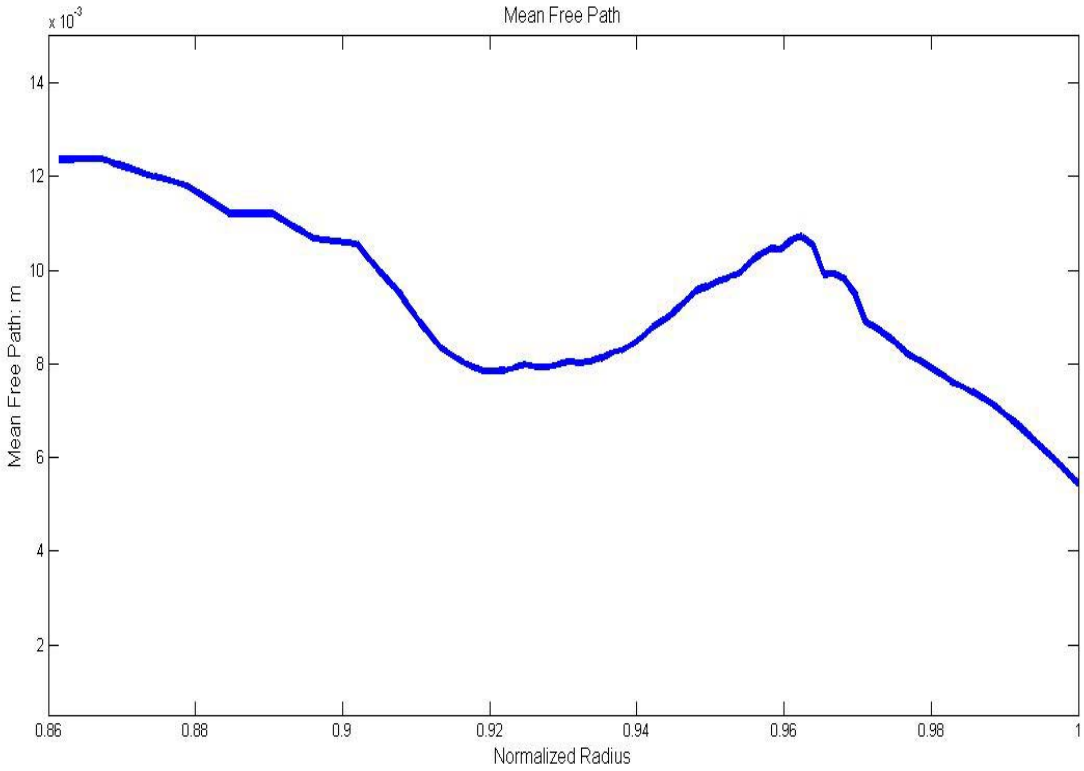

Interval Size Sensitivity

- Below is a plot showing the change in the calculated density as interval width is decreased from near the minimum mean free

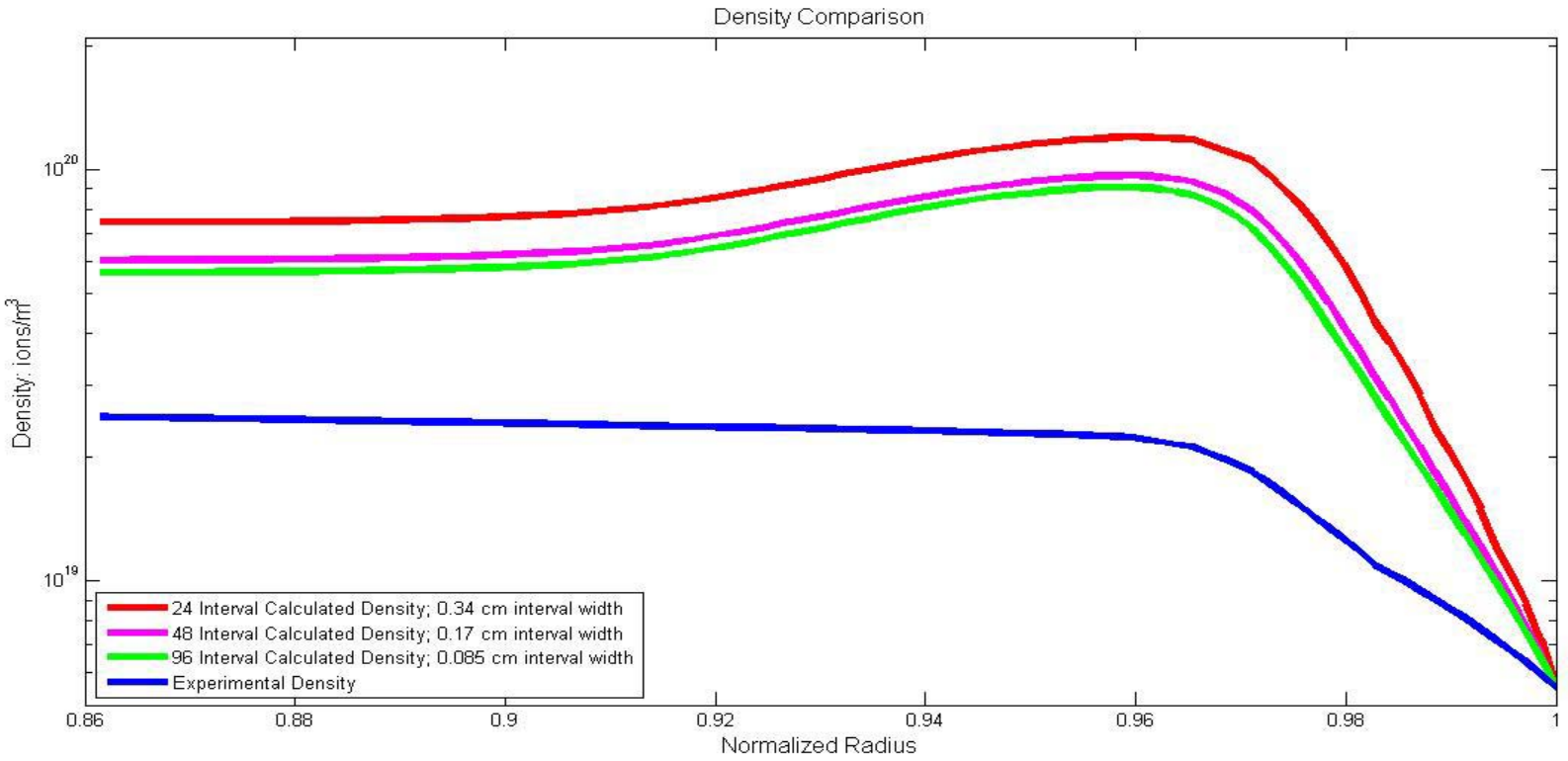

Boundary Conditions

- A global particle balance including a neutral recycling calculation was performed to obtain the ion particle flux crossing the separatrix, which was used as a boundary condition

- The neutral recycling calculation is not exactly certain, and the results are shown for the increase of the neutral recycling flux by 50% and 100% below, decreasing the discrepancy with experiment

Modified Neutral Recycling Flux

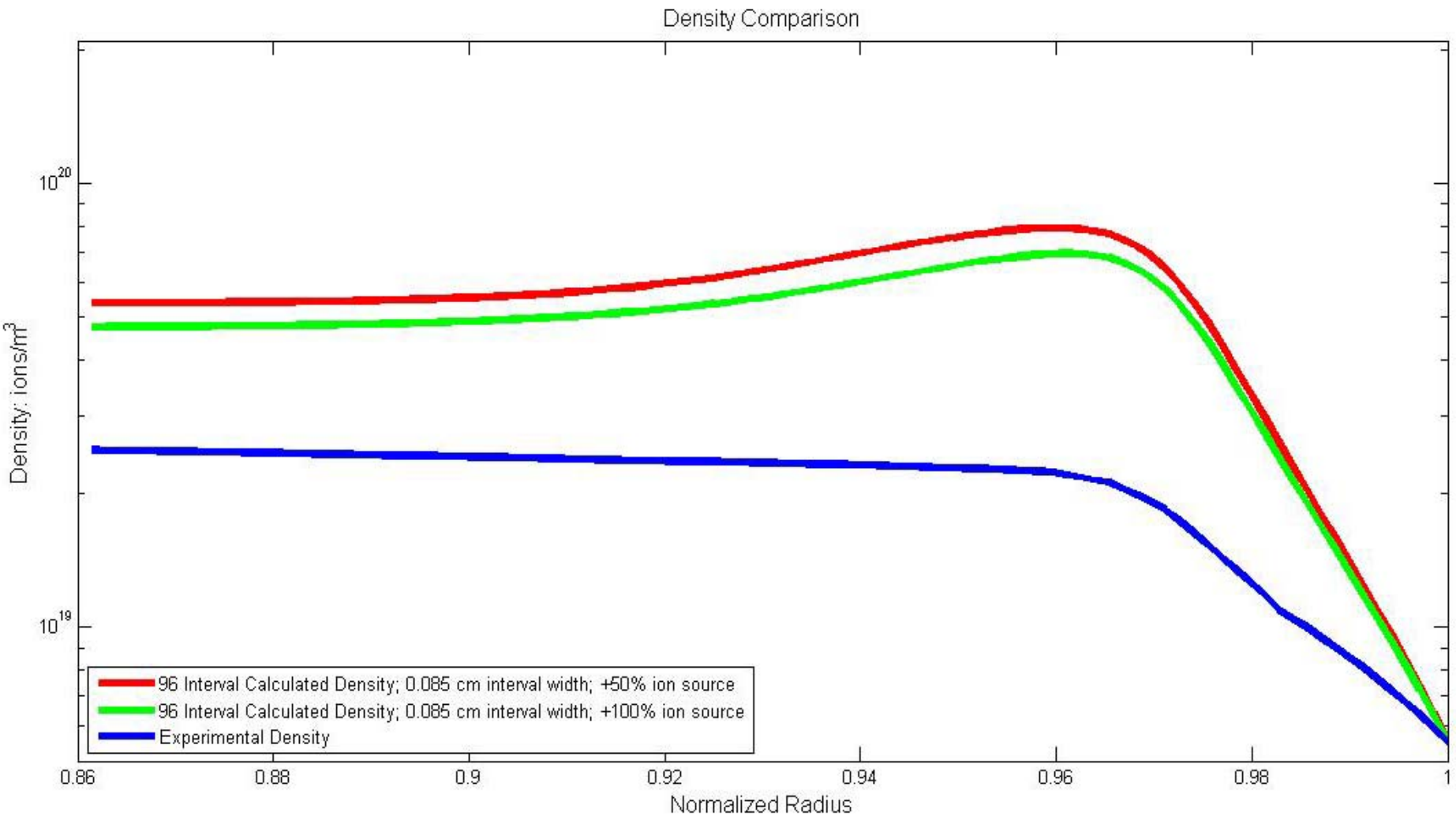

Conclusions

- This work is currently ongoing
- Continued investigations of the numerical solution of the generalized diffusion equations will be carried out
- Continued investigations of effects of uncertainties on solution will be carried out

References

- 1. Stacey, W. M. “Ion Particle Transport in the Tokamak Edge Plasma.” Contributions to Plasma Physics. 48.1-3 (2008): 94-98

- 2. W. M. Stacey and R. J. Groebner. “Interpretation of Particle Pinches and Diffusion Coefficients in the Edge Pedestal of DIII-D H-Mode Plasmas.” Physics of Plasmas. 16, 102504 (2009).

SABR

SUBCRITICAL ADVANCED BURNER REACTOR

W. M. STACEY

Georgia Tech

APS-DPP Atlanta

November, 2009

MOTIVATION FOR TOKAMAK FUSION-FISSION HYBRID TRANSMUTATION REACTOR

- The growing stockpile of discharged LWR fuel is an impediment to the world-wide expansion of carbon free nuclear power.
- Separating and burning the actinides would dramatically reduce the required number and lifetime of geological HLW repositories for spent nuclear fuel.
- Pure fission burner reactors and separations facilities could be deployed for this purpose over about 2030-2080, but studies indicate some reactors should be subcritical to achieve deep actinide burnup.
- A large worldwide R&D effort is supporting the leading tokamak magnetic fusion concept, and ITER will demonstrate the fusion physics and technology needed for a hybrid over 2018-2030, although high reliability, steady-state operation must be achieved.
- A series of studies has been performed at Georgia Tech to evaluate combining ITER fusion physics and technology with the leading Na-cooled, metal-fuel fast burner reactor technology to design a fusion-fission hybrid burner (transmutation) reactor.

SUB-CRITICAL ADVANCED BURNER REACTOR (SABR)

- **ANNULAR FAST REACTOR (3000 MWth)**

1. Fuel—TRU from spent nuclear fuel. TRU-Zr metal being developed by ANL.
2. Sodium cooled, loop-type fast reactor.
3. Based on fast reactor designs being developed by ANL in DoE Nuclear Program.

- **TOKAMAK D-T FUSION NEUTRON SOURCE (200-500 MWth)**

1. Based on ITER plasma physics and fusion technology.
2. Tritium self-sufficient (Li_4SiO_4).
3. Sodium cooled.

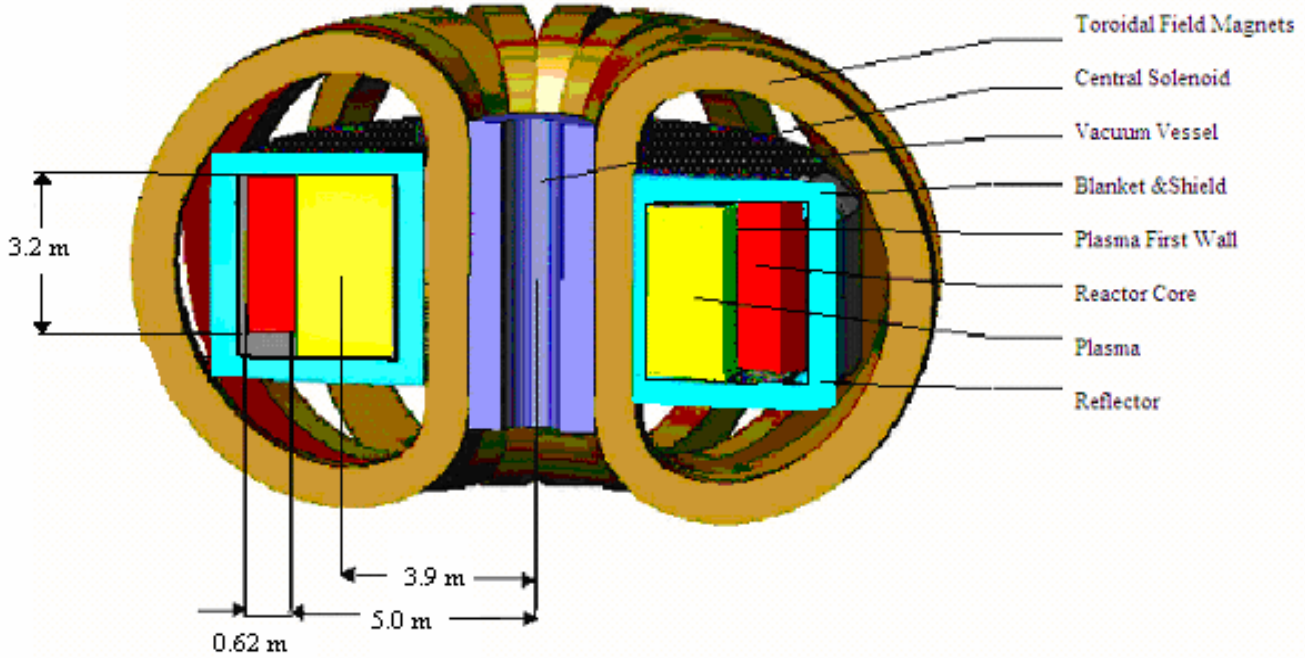

FUEL

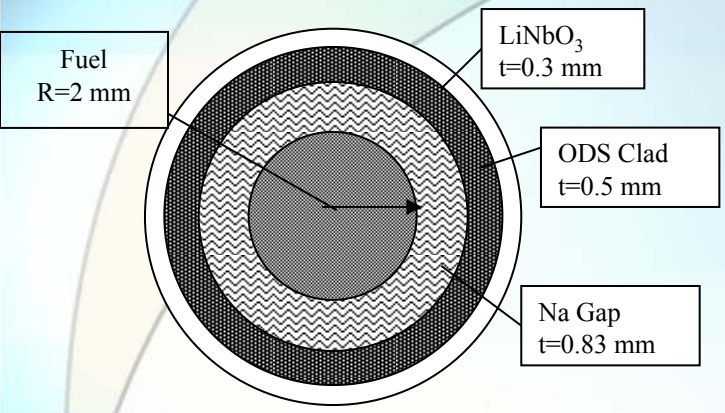

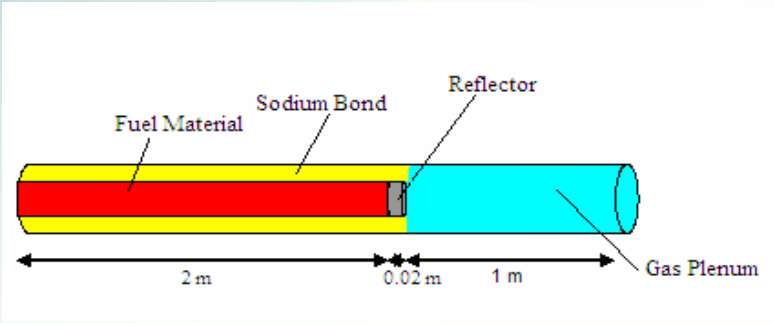

Axial View of Fuel Pin

Composition 40Zr-10Am-10Np-40Pu (w/o)
(Under development at ANL)

Design Parameters of Fuel Pin and Assembly

Length rods (m)	3.2	Total pins in core	248778
Length of fuel material (m)	2	Diameter_Flats (cm)	15.5
Length of plenum (m)	1	Diameter_Points (cm)	17.9
Length of reflector (m)	0.2	Length of Side (cm)	8.95
Radius of fuel material (mm)	2	Pitch (mm)	9.41
Thickness of clad (mm)	0.5	Pitch-to-Diameter ratio	1.3
Thickness of Na gap (mm)	0.83	Total Assemblies	918
Thickness of $LiNbO_3$ (mm)	0.3	Pins per Assembly	271
Radius Rod w/clad (mm)	3.63	Flow Tube Thickness (mm)	2
Mass of fuel material per rod (g)	241	Wire Wrap Diameter (mm)	2.24
$Volume_{Plenum}$ / $Volume_{fm}$	1	Coolant Flow Area/ assy (cm^2)	75

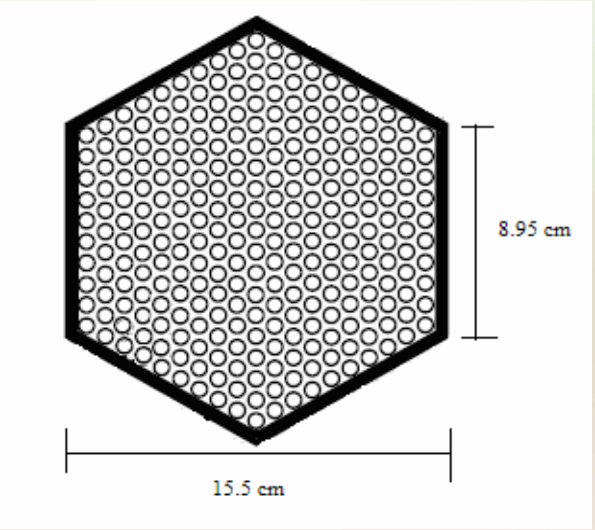

Cross-Sectional View Fuel Assembly

4-BATCH FUEL CYCLE

- Fuel cycle constrained by 200 dpa clad radiation damage lifetime. 4 (700 fpd) burn cycles per residence
- OUT-to-IN fuel shuffling
- BOL k_{eff} = 0.972, P_{fus} = 75MW, 32 MT TRU
- BOC k_{eff} = 0.894, P_{fus} = 240MW, 29 MT TRU
- EOC k_{eff} = 0.868, P_{fus} = 370MW, 27 MT TRU
- 24% TRU burnup per 4-batch residence, >90% with repeated recycling
- 1.05 MT TRU/FPY fissioned
- Supports 3.0 1000 MWe LWRs (0.25 MT TRU/yr) at 76% availability during operation (2 mo refueling).

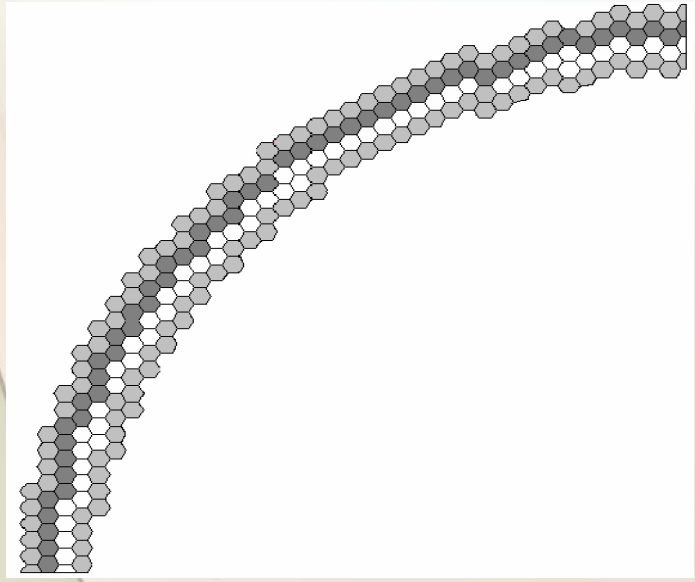

ANNULAR CORE CONFIGURATION

SABR TRU FUEL COMPOSITION (w/o)

Isotope	Fresh Fuel	To Re-Process	Core Av EOC/BOC
Np-237	17.0	7.25	9.1/8.3
Pu-238	1.4	17.3	14.6/17.3
Pu-239	38.3	18.3	21.9/20.3
Pu-240	17.3	29.2	27.2/28.2
Pu-241	6.5	7.31	5.55/5.55
Pu-242	2.6	7.45	6.50/6.99
Am-241	13.63	7.45	8.87/8.35
Am-242m	0.00	0.84	0.71/0.74
Am-243	2.8	2.79	2.82/2.85
Cm-242	0.00	0.59	0.33/0.35
Cm-243	0.00	0.10	.075/.080
Cm-244	0.00	2.51	2.01/2.24
Cm-245	0.00	0.56	0.42/0.49

Neutron Source Design Parameters

SABR TOKAMAK NEUTRON SOURCE PARAMETERS

Parameter	**Nominal SABR**	**Extended SABR**	**ITER**	**Pure Fusion Electric ARIES-AT**
Current, I (MA)	8.3	10.0	15.0	13.0
P_{fus} (MW)	180	500	400	3000
Major radius, R (m)	3.75	3.75	6.2	5.2
Magnetic field, B (T)	5.7	5.7	5.3	5.8
Confinement $H_{IPB98}(y,2)$	1.0	1.06	1.0	1.7
Normalized beta, β_N	2.0	2.85	1.8	5.4
Plasma Mult., Q_p	3	5	5-10	>30
H&CD Power, MW	100	100	110	
NeutronΓ_n (MW/m²)	0.6	1.8	0.5	4.9
FW q_{fw} MW/m²)	0.23	0.65	0.5	1.2
Availability (%)	76	76	10 ?	>90

ADAPTED ITER NEUTRON SOURCE TECHNOLOGY

- Six 20 MW ITER LHR launchers.
- Adapted ITER FW and divertor for Na and He coolant. Replaced SS with ODS steel. Confirmed heat removal with FLUENT code.
- FW lifetime 6.5 FPY at 200 dpa. Replace every 3rd refueling shutdown.
- Scaled down ITER SC CS and TF magnet designs, maintaining ITER standards.
- Multilayer shield. MCNP and EVENT predict > 30 FPY (40 yrs @ 75% avail) radiation damage lifetime for SC magnets.

Li_4SiO_4 Tritium Breeding Blanket

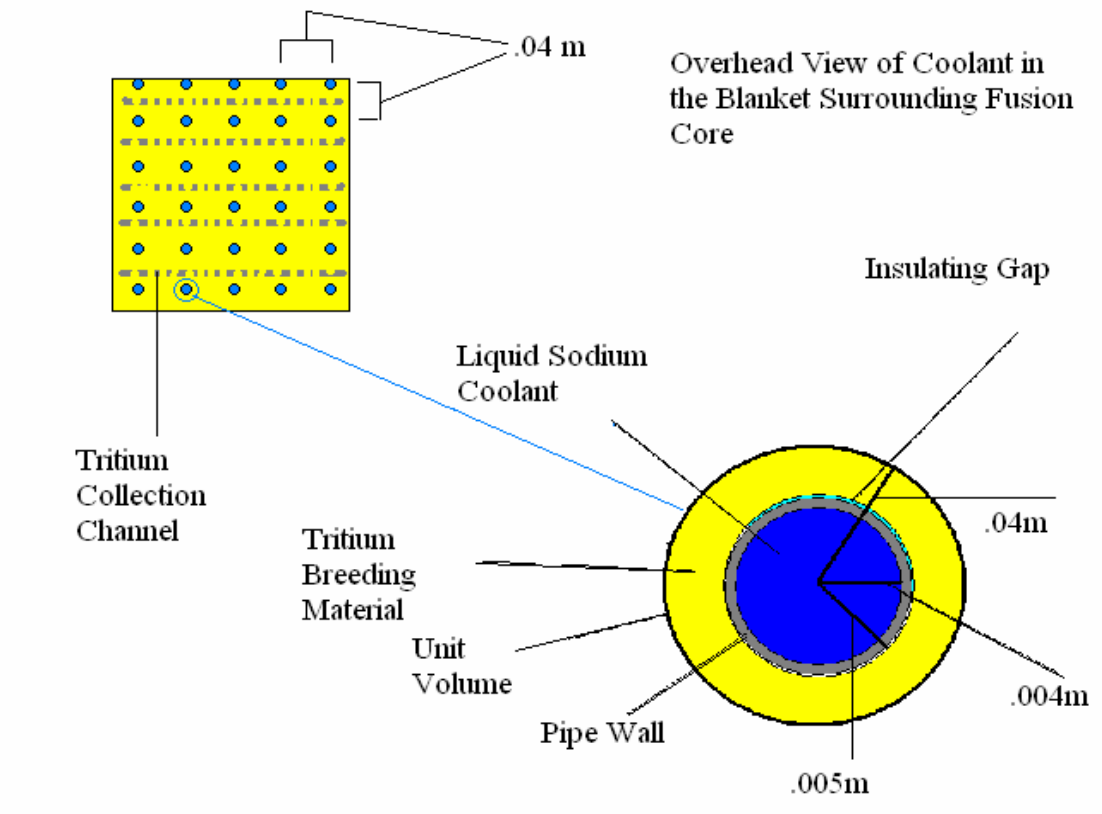

15 cm Thick Blanket Around Plasma (Natural LI) and Reactor Core (90% Enriched LI) Achieves TBR = 1.16.

NA-Cooled to Operate in the Temperature Window 420-640 C.
Online Tritium Removal by He Purge Gas System.

Dynamic ERANOS Tritium Inventory Calculations for 700 d Burn Cycle, 60 d Refueling Indicated More Than Adequate Tritium Production.

CONCLUSIONS

- The physics and technology *performance parameters of ITER* (many of which have been achieved already) will be *more than adequate* for a fusion neutron source for a FFH transmutation reactor. ITER will be the prototype.
- *Additional R&D* will be needed to obtain greater component and plasma *reliability* than demanded of ITER, *tritium breeding technology*, and a more radiation resistant *structural material*.
- The physics performance parameters and FW neutron and heat loads for a FFH are significantly *less than are required for pure fusion electric power.*
- The feasibility of *deployment* of a tokamak fusion neutron source, based on ITER physics and technology, in a FFH transmutation reactor *by about 2040* is *compatible* with the *nuclear power scenario* for deploying transmutation reactors over roughly *2030-2080.*
- Thus, *FFH transmutation reactors* (for the fissioning of the transuranics in discharged LWR fuel and hence the reduction of geological waste repository requirements) would seem to be the target of opportunity for *fusion to contribute to solving the world's energy problems starting in the first half of the present century.*

R-Z Cross section SABR calculation model

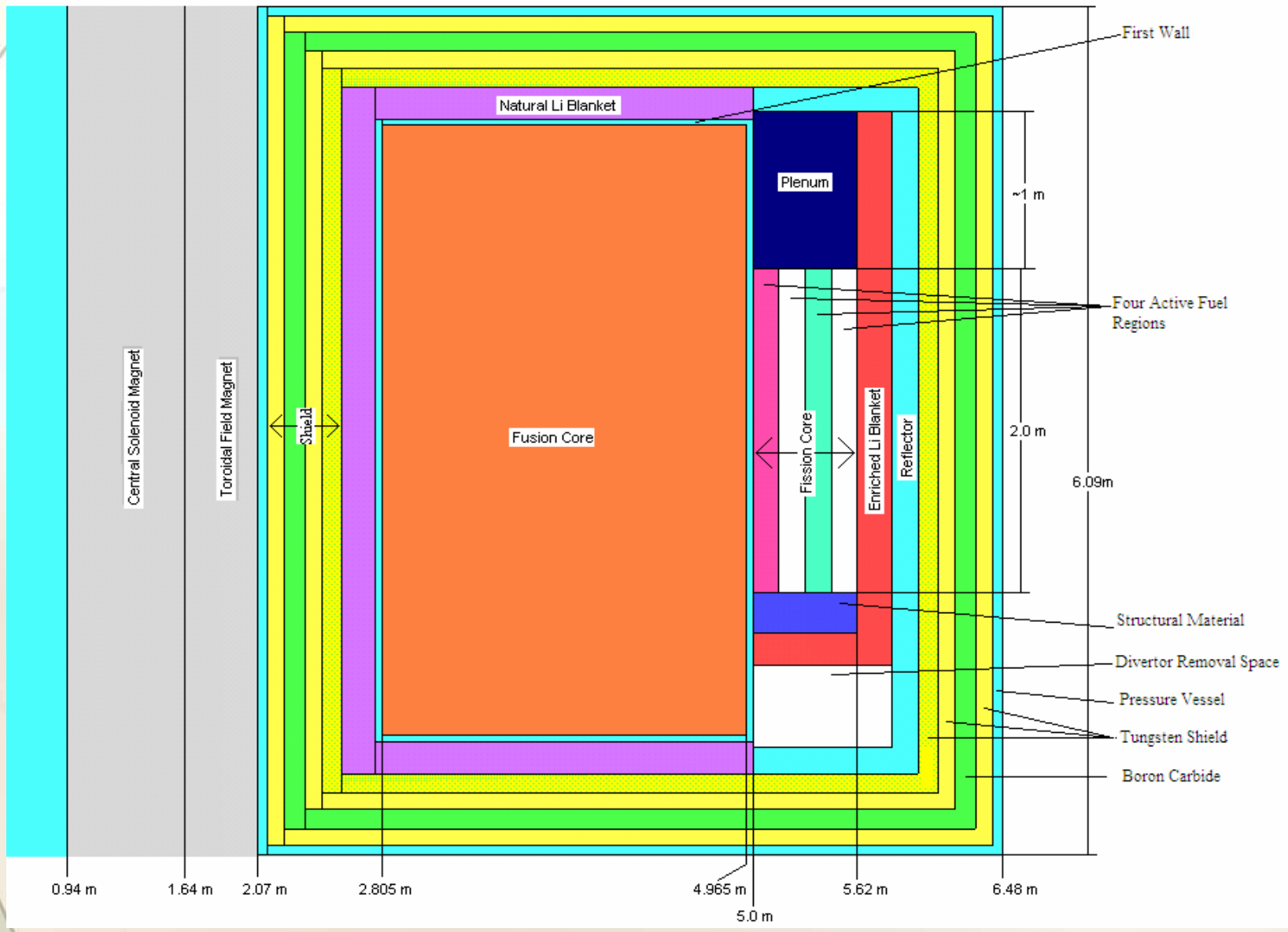

R&D FOR A TOKAMAK FFH NEUTRON SOURCE IS ON THE PATH TO PURE FUSION ELECTRIC POWER

FUSION R&D FOR A TOKAMAK F-F HYBRID

1. **Ongoing worldwide tokamak physics R&D program, including ITER-specific issues (e.g. ELM suppression, startup scenarios).**
2. **ITER construction and operation experience-- prototype.**
3. **Physics R&D on reliable steady-state, disruption-free operation, burn control, etc.**
4. **Plasma Support Technology (magnets, heating systems, etc.) R&D for component reliability.**
5. **Remote Maintenance.**
6. **Fusion Nuclear Technology (tritium breeding, etc.) R&D**
7. **Advanced Structural Materials (200 dpa) R&D**

FURTHER FUSION R&D FOR TOKAMAK ELECTRIC POWER

8. **Advanced confinement and pressure limits physics R&D.**
9. **Advanced DEMO.**

SABR FUEL CYCLE

C. M. Sommer, W. M. Stacey, B.Petrovic,
Georgia Tech
November, 2009

Promise of FFH transmutation reactors:

- Longer fuel residence time limited by radiation damage, not criticality.
- Larger TRU fuel fraction, not limited by TRU β.

SUB-CRITICAL ADVANCED BURNER REACTOR (SABR)

ANNULAR FAST REACTOR

1. Fuel—TRU from spent nuclear fuel. TRU-Zr metal being developed by ANL.
2. Sodium cooled, loop-type fast reactor.

Based on fast reactor designs being developed by ANL in DoE Nuclear Program.

TOKAMAK D-T FUSION NEUTRON SOURCE

1. Based on ITER plasma physics and fusion technology.
2. Tritium self-sufficient (Li_4SiO_4).
3. Sodium cooled.

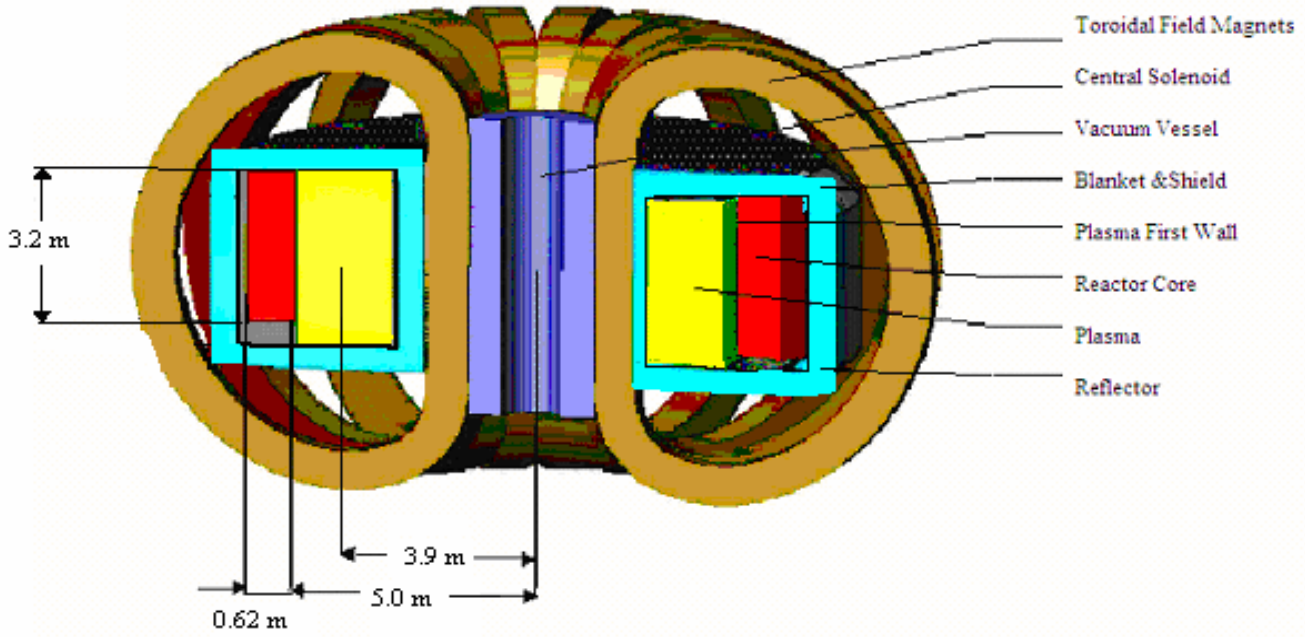

Fuel Cycle Analysis of SABR

- Purpose: To find a fuel cycle capable of transmuting greater than 90% of the TRU from LWR's
- Several reprocessing fuel cycles were analyzed based on a fuel residence time limited by the radiation damage limit to structural materials
- Once through cycle was analyzed to determine the feasibility of a deep burn

SABR Model

- Eranos Model of SABR
  - RZ Geometry
  - 33 Energy Groups ranging from 0.1 eV to 20 MeV
  - Solved using discrete ordinates theory
  - 4 region annular fission core
  - 14 MeV neutron source inside the plasma region
- Reprocessing fuel cycles simulated
  - 100 dpa, 200 dpa, 300 dpa

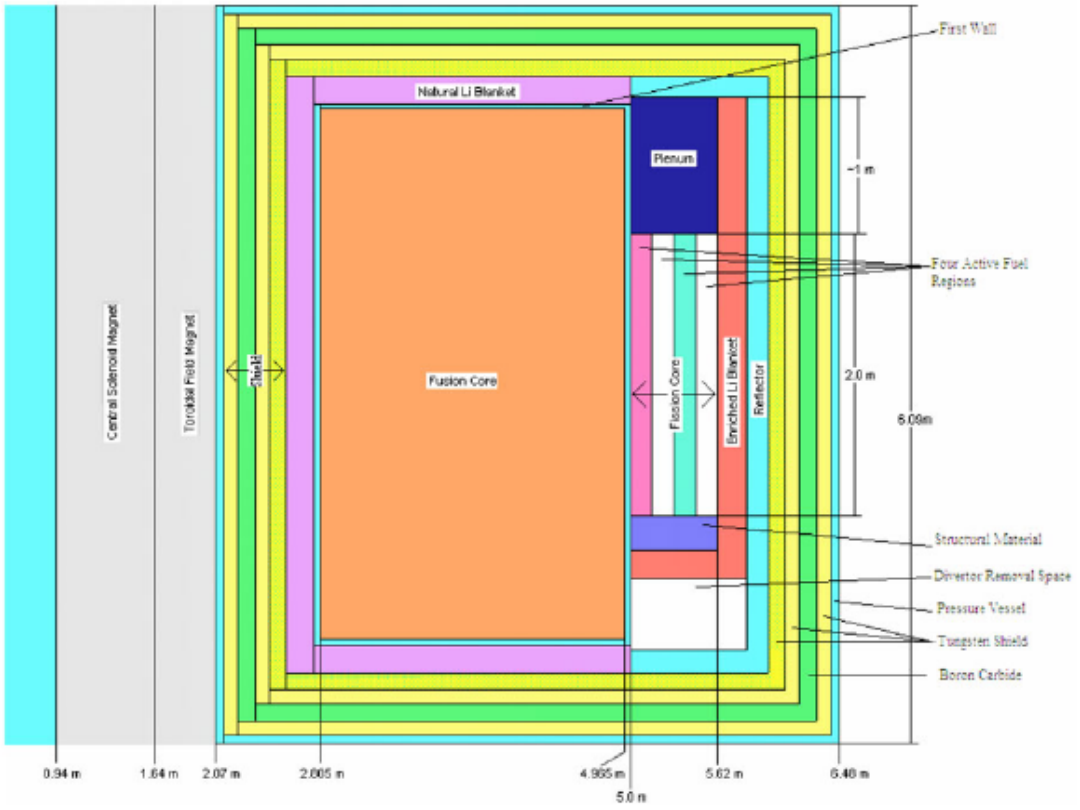

SABR Fuel Design

	Mass percent
Isotope	Beginning of life (BOL)
^{237}Np	17.0
^{238}Pu	1.4
^{239}Pu	38.8
^{240}Pu	17.3
^{241}Pu	6.5
^{242}Pu	2.6
^{241}Am	13.6
^{243}Am	2.8

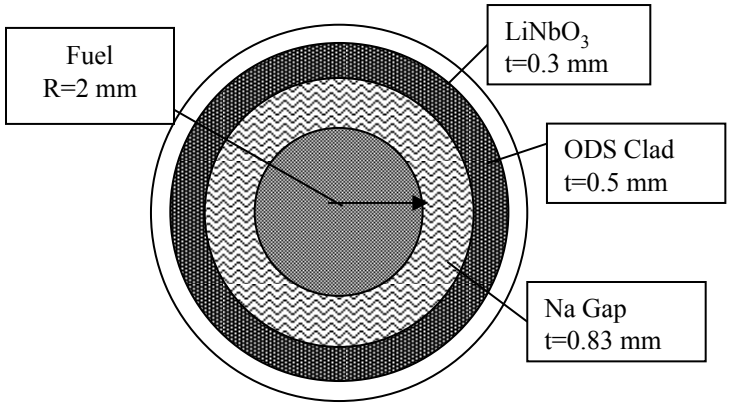

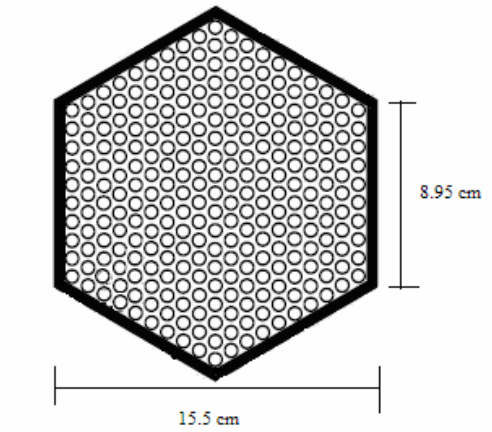

SABR FUEL CYCLE

SABR Fuel Assembly

SABR Fuel Cycle

- Four fuel cycles analyzed
  - 100 dpa, 350 full power day burn cycle with reprocessing
  - 200 dpa, 700 full power day burn cycle with reprocessing
  - 300 dpa, 1000 full power day burn cycle with reprocessing
  - Once Through Cycle deep burn approximately 90%
- Pyrometallurgical Reprocessing used
  - 99% Recovery Rate of TRU
  - 1% Fission product contamination of reprocessed fuel

SABR Fuel Cycle

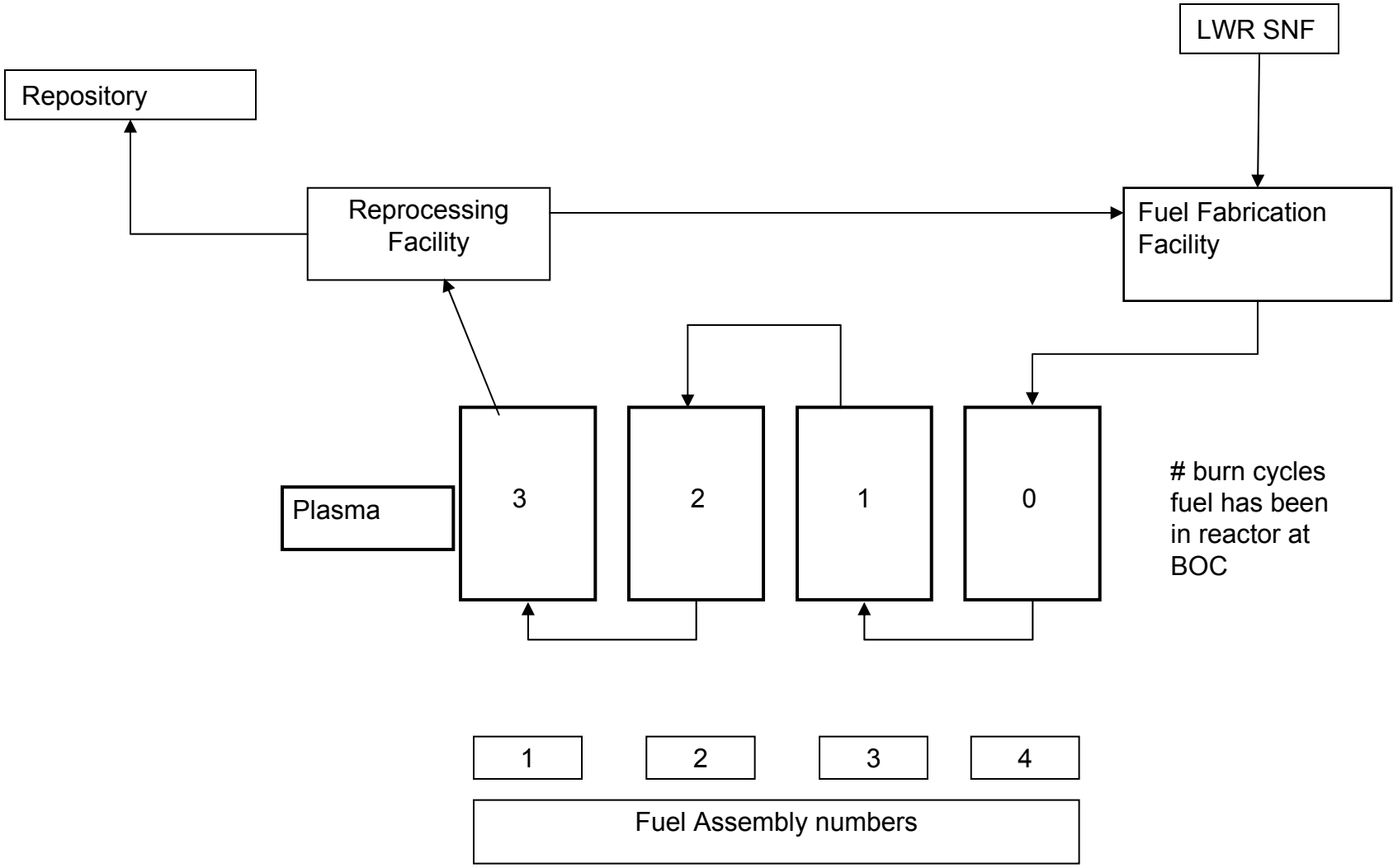

Fuel Cycle Performance

Parameter	Units	
Cycle		200 dpa
Burn Cycle Length Time	FPD	700
4 Batch Residence Time	FPY	7.67
K_{eff}(BOL/BOC/EOC)		0.972/0.894/ 0.868
P_{fus}(BOL/BOC/EOC)	MW	75/240/370
TRU Content (BOC/EOC)	MT	29.0/27.1
Power Peaking (BOC/EOC)		1.80/1.98
TRU Burned per Residence	% kg	23.8% 1900
TRU Burned per Year	MT/FPY	1.05
LWR Support Ratio		3.54
Average Core Flux Across Cycle	n/cm^2-s	4.81E15
TRU to Repository	kilograms	31.4

SABR Power Distribution

- Highly peaked power distribution in the inner fuel regions
- Only fuel shuffling accounted for
- Power peaking less than 2.0

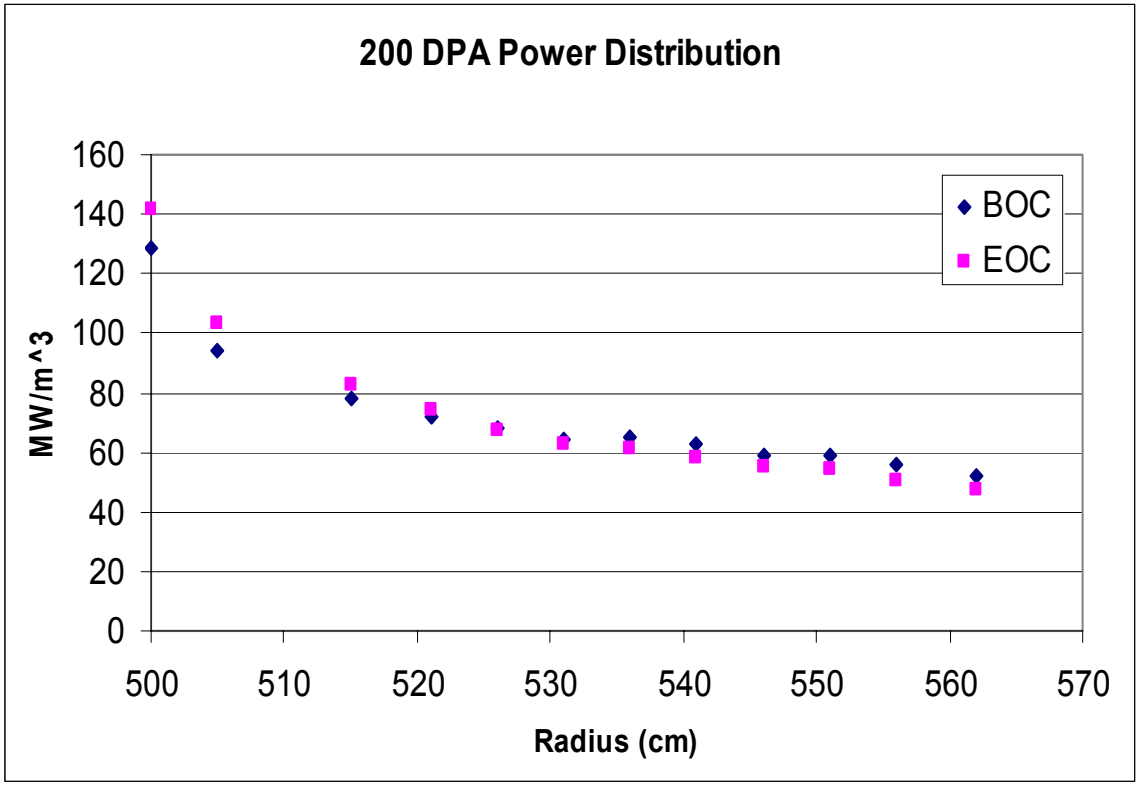

Decay Heat to the Repository

- Long term integral decay heat limiting repository factor
- Reduction of long term decay heat by transmutation of TRU
- Higher burnup → less TRU in repository

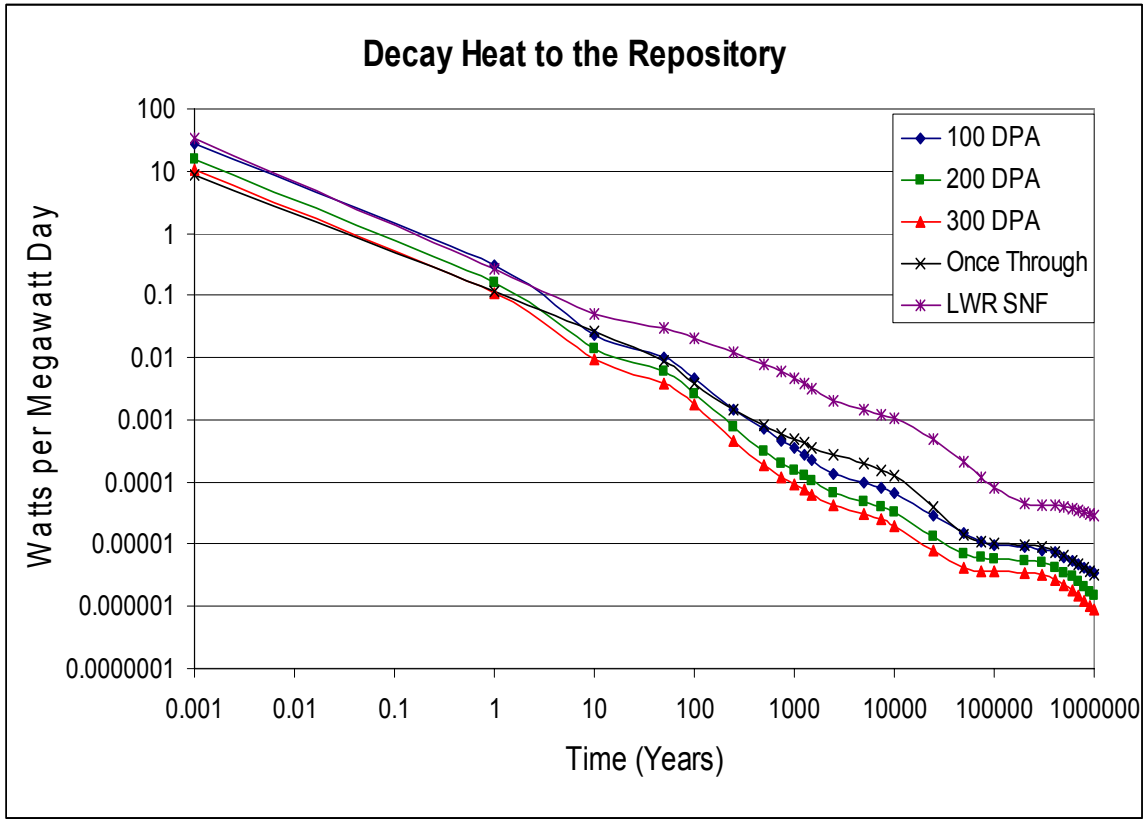

Summary

- 76% Availability → 3.0 LWR's supported by SABR
- Greater than 90% burnup can be achieved in SABR
- TRU to the repository dependent on burnup and separation efficiency in reprocessing method
- Once through cycle is not feasible

Fuel Cycle Performance

Parameter	Units				
Cycle		100 dpa	200 dpa	300 dpa	OTC
Burn Cycle Length Time	FPD	350	700	1000	4550
4 Batch Residence Time	FPY	3.83	7.67	10.95	49.8
K_{eff}(BOC/EOC)		0.940/ 0.916	0.894/ 0.868	0.887/ 0.834	0.784/ 0.581
P_{fus}(BOC/EOC)	MW	155/218	240/370	286/461	1012/1602
TRU Content (BOC/EOC)	MT	29.6/28.6	29.0/27.1	28.3/25.4	22.6/9.5
Power Peaking (BOC/EOC)		1.68/1.78	1.80/1.98	1.82/2.04	1.97/1.59
TRU Burned per Residence	%	16.7%	23.8%	31.6%	87.2%
TRU Burned per Year	MT/FPY	1.04	1.05	1.05	1.05
LWR Support Ratio		3.27	3.54	3.62	3.82
Average Core Flux Across Cycle	n/cm^2-s	4.73E15	4.81E15	5.28E15	1.82E16
TRU to Repository	kilograms	67.7	34.4	19.7	87.4

SABR Power Distribution

- Highly peaked power distribution in the inner fuel regions
- Longer residence time in reprocessing cycles higher power peaking
- OTC EOC lower power peaking

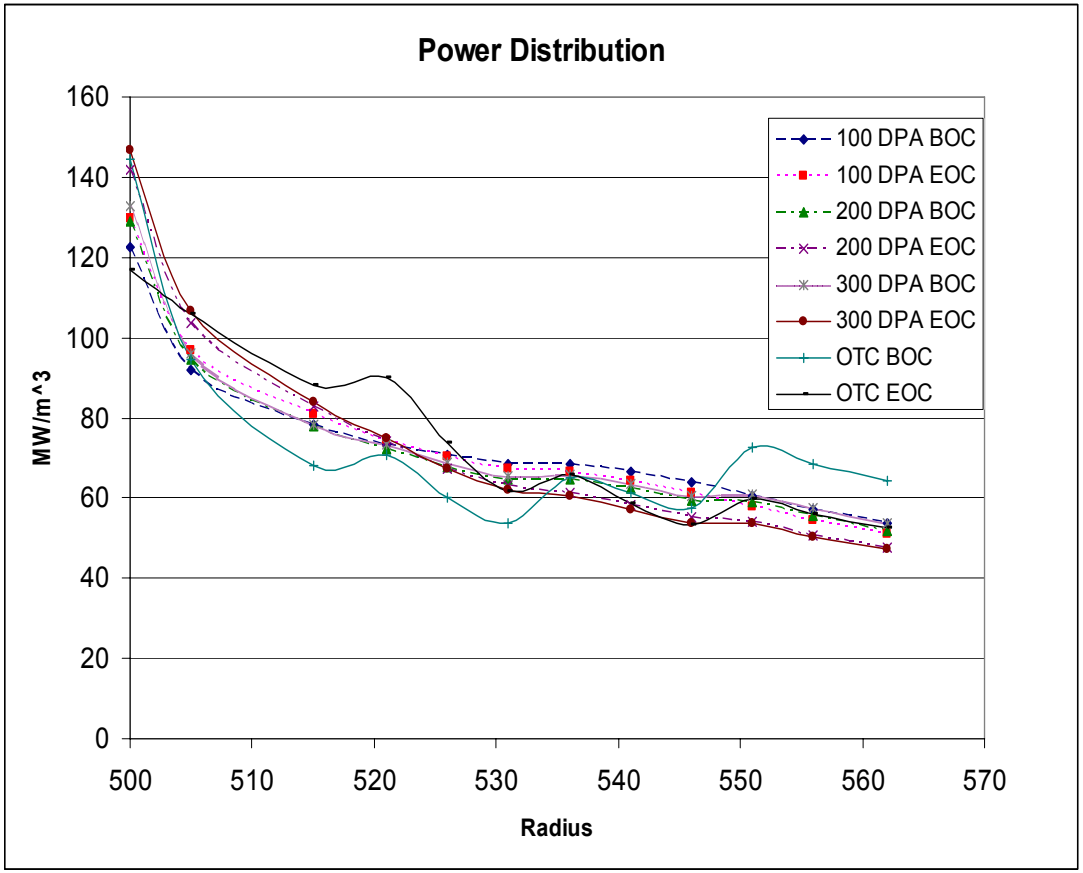

A Safety and Dynamics Analysis of SABR

T. S. Sumner, W. M. Stacey and S. M. Ghiaasiaan

Georgia Tech

November , 2009

SUB-CRITICAL ADVANCED BURNER REACTOR (SABR)

ANNULAR FAST REACTOR

1. Fuel—TRU from spent nuclear fuel. TRU-Zr metal being developed by ANL.
2. Sodium cooled, loop-type fast reactor.

Based on fast reactor designs being developed by ANL in DoE Nuclear Program.

TOKAMAK D-T FUSION NEUTRON SOURCE

1. Based on ITER plasma physics and fusion technology.
2. Tritium self-sufficient (Li_4SiO_4).
3. Sodium cooled.

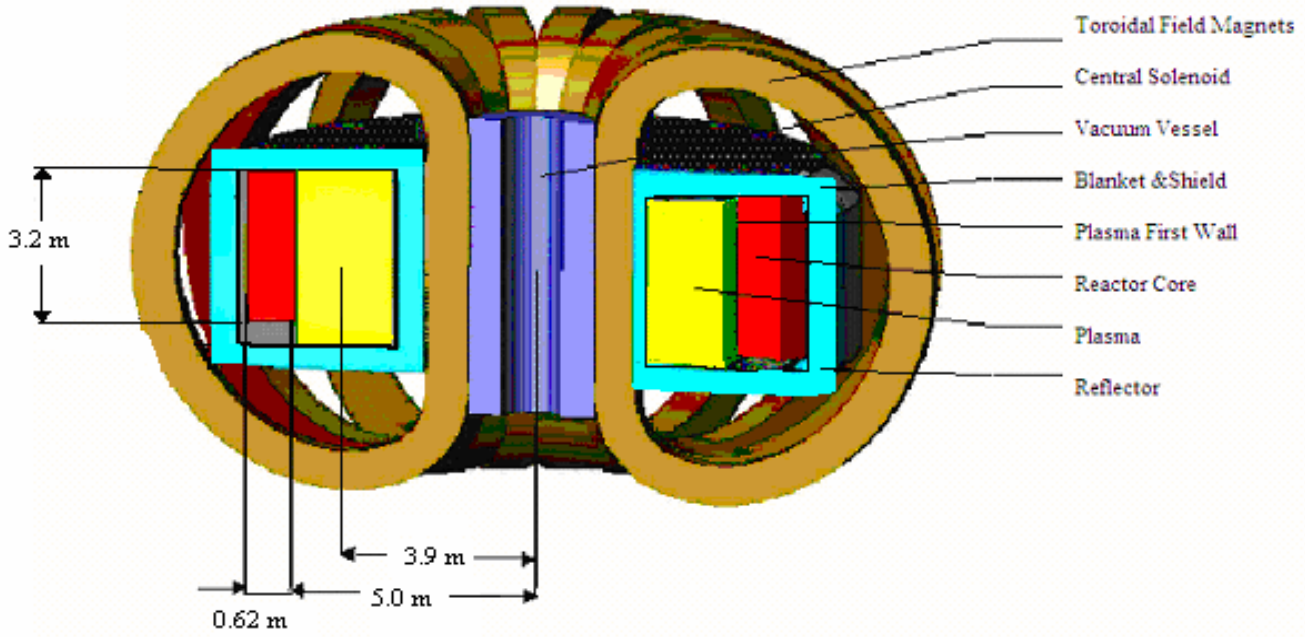

Safety and Dynamics Analysis of SABR

- Purpose: To find the transient response of the subcritical, sodium-cooled, TRU-fueled, fast transmutation reactor design concept.
- Several initiating accidents were simulated to determine the magnitude of each accident that could be tolerated without resulting in permanent damage to the fission core.
- How much time would be available to take corrective measures to prevent damage to the reactor?

Thermal Hydraulics Model

- Coupled fission core power level with the thermal hydraulics of the thermal heat removal system using RELAP5-3D.
- Fusion neutron source accounted for by the source term in the point kinetics equations.
- ATHENA version of RELAP5-3D allows for liquid metal coolants.

Thermal Hydraulics Model, continued…

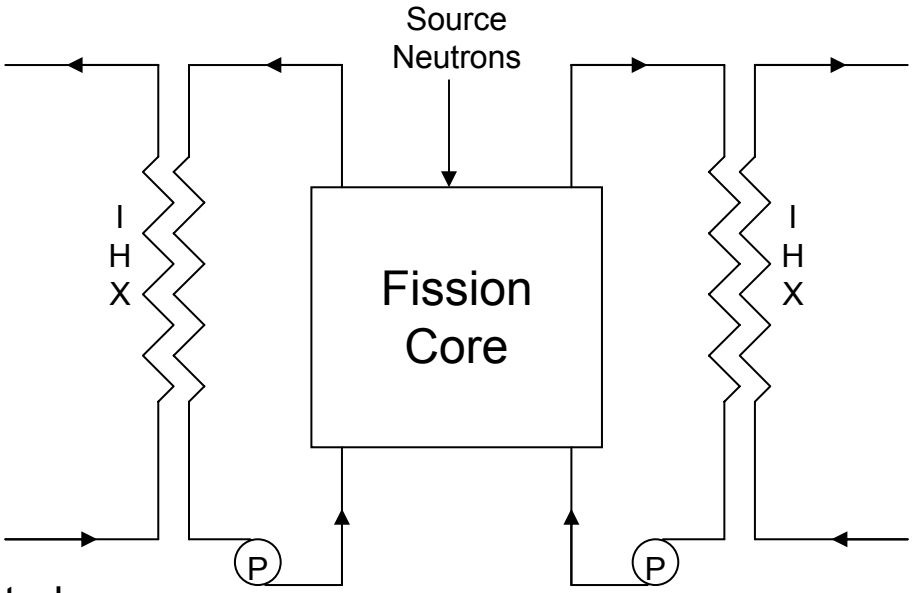

- Accidents simulated:
  - Loss of Power Accident (LOPA),
  - Loss of Flow Accident (LOFA),
  - Loss of Heat Sink Accident (LOHSA), and
  - Accidental Increase in Fusion Neutron Source Strength.
- Coolant Boiling Temperature: 1,156 K
- Fuel Melting Temperature: 1,473 K

LOPA

- A Loss of Power Accident results in zero power to SABR's auxiliary systems.
  - All sodium coolant pumps shut off,
  - Heating power to the plasma is lost

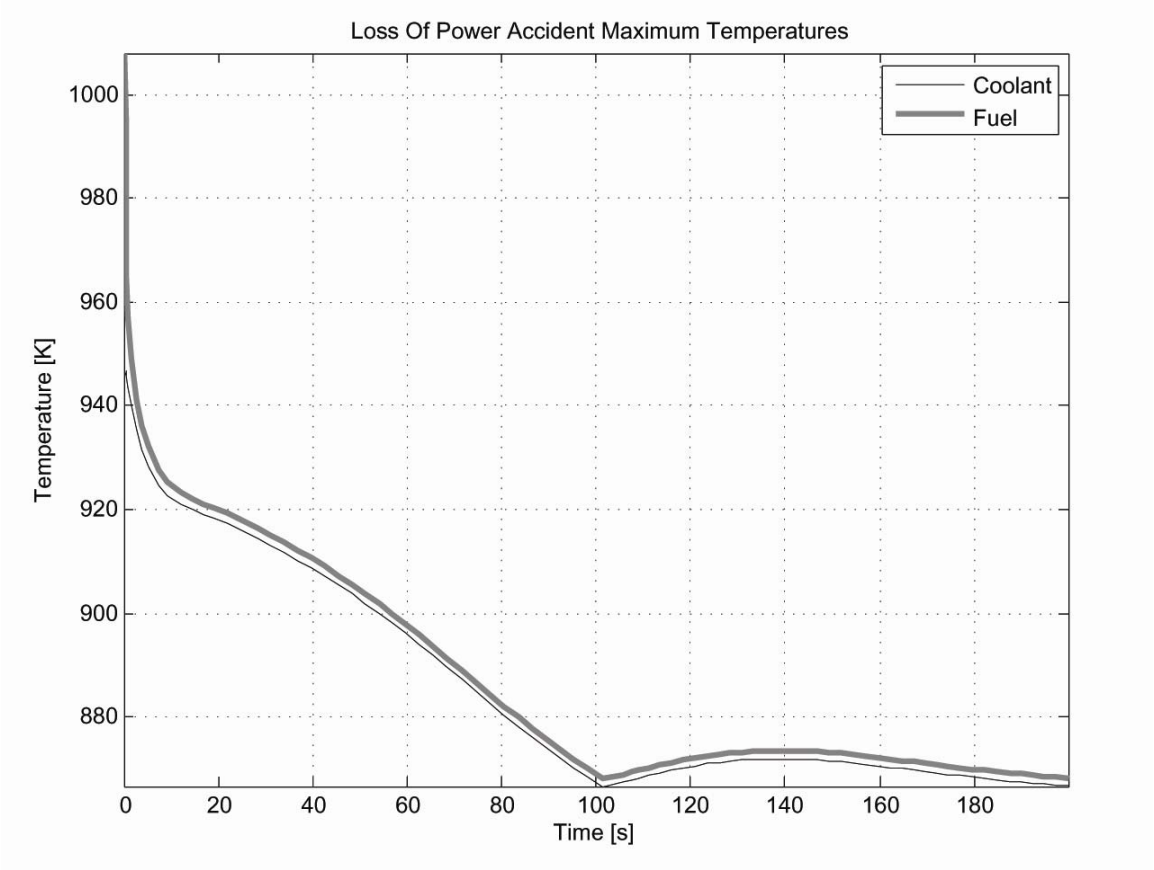

LOFA

- A Loss of Flow Accident results in one or more of the primary coolant loop pumps failing. (neutron source remains on)

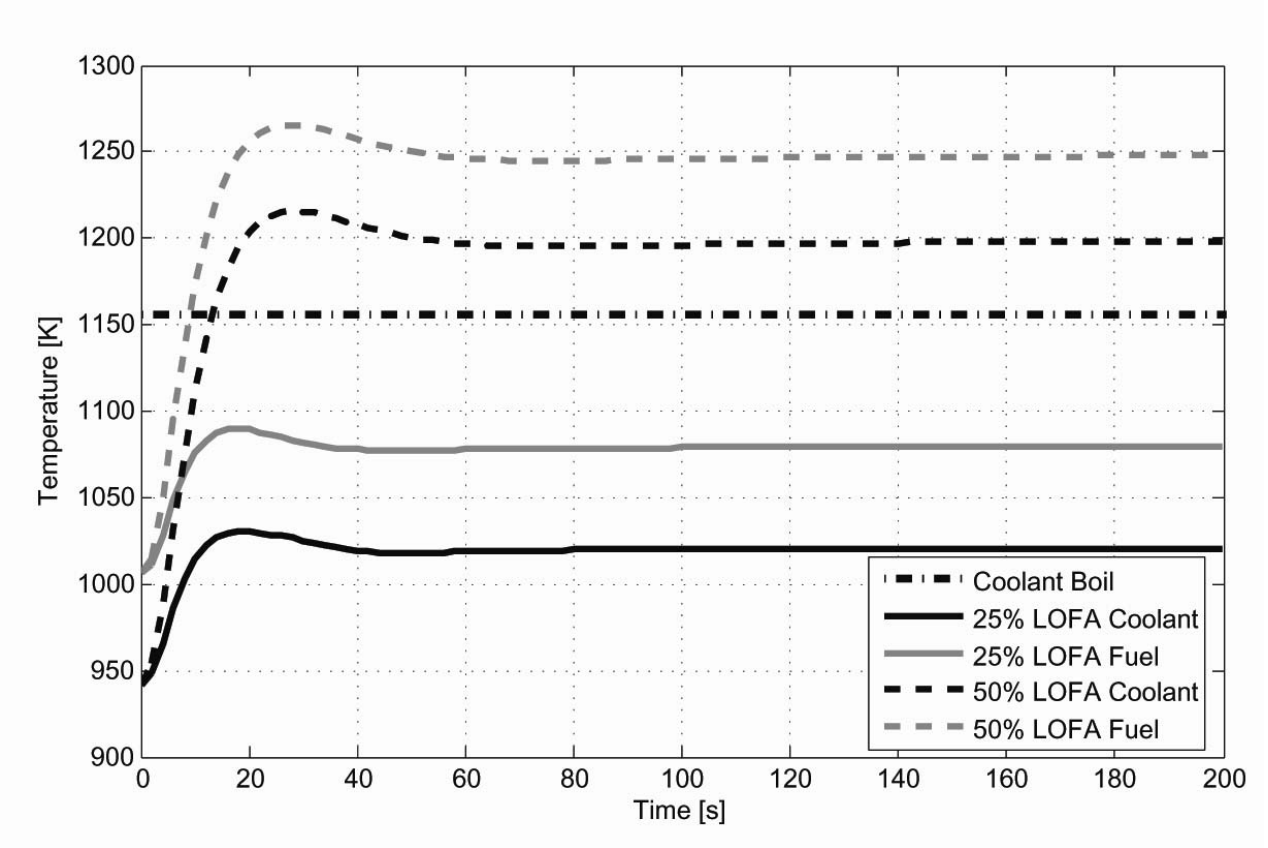

LOHSA

- A Loss of Heat Sink Accident was modeled as the failure of the intermediate coolant loop EM pumps. (Neutron source remains on)

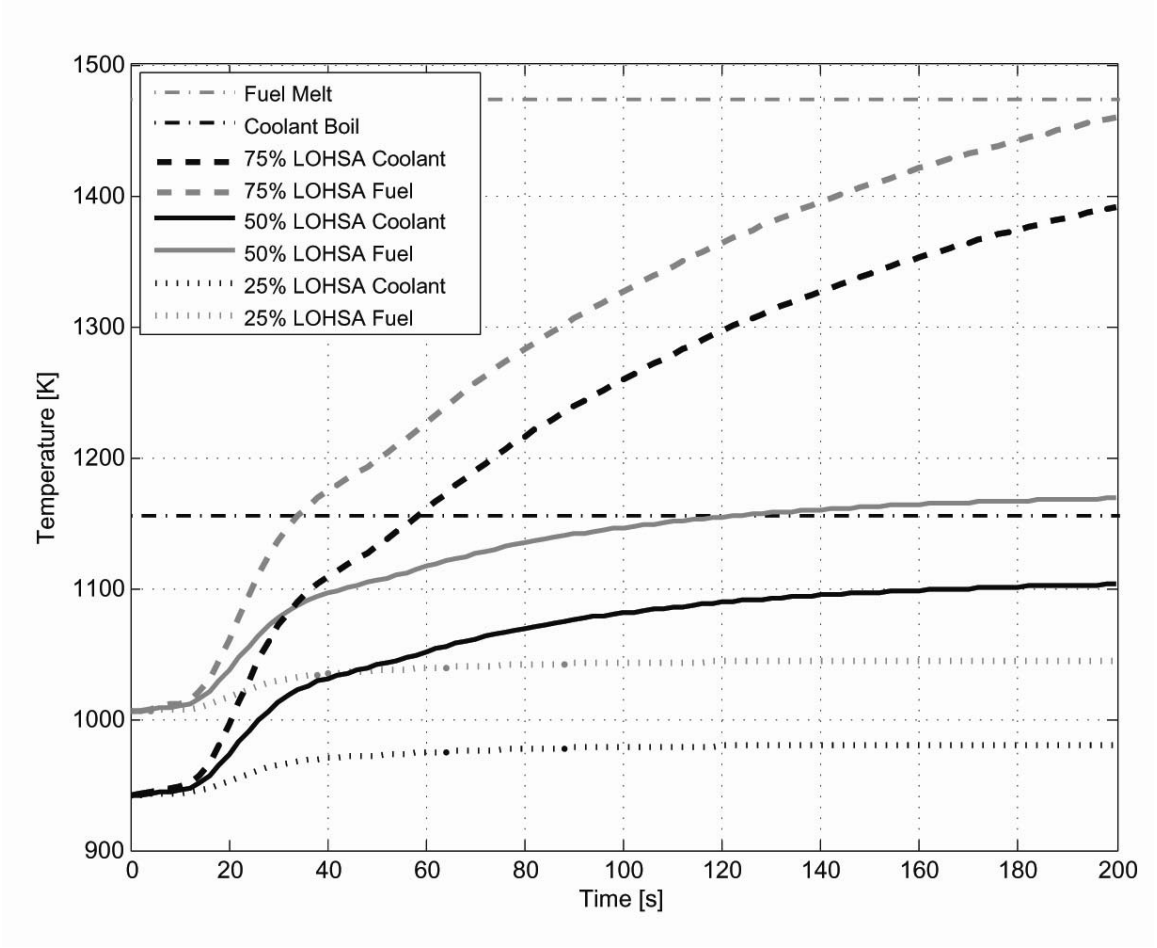

Accidental Increase in Fusion Neutron Source Strength

- What is the maximum allowable fusion neutron source strength increase that could be tolerated before either coolant boiling or fuel melting occurs?

	BOL	BOC	EOC
Steady-state Fusion Power Level (MW)	73	242	370
Fusion Power Leading to Coolant Boiling (MW)	121.2	398.1	563.9
Maximum Tolerable Increase in Fusion Power (MW)	48	156	194
Maximum Fuel Temperature (K)	1265	1336	1337
(Note: Coolant boiling occurs at 1,156 K and fuel melting occurs at 1,473 K)			

- Above fusion neutron source strength increases resulting in coolant boiling would surpass the Troyon Beta Limit and terminate the source excursion.

Summary

- Fission core power can be reduced to decay heat levels in a couple of seconds without source neutrons
- SABR is safe against LOPA
- SABR can tolerate up to 50% LOFA and LOHSA without sustaining permanent core damage
- Accidental increases in neutron source strength could be limited by operation near inherent density and beta limits.

REPRESENTATION OF THE PLASMA FLUID EQUATIONS IN MILLER EQUILIBRIUM FLUX SURFACE GEOMETRY

W. M. Stacey and Cheonho Bae
Georgia Tech
November, 2009

The "natural" coordinate systems for tokamak plasma physics computations is the set of nest magnetic flux surfaces. In general applications, these flux surface coordinate system must be determined by numerically solving the Grad-Shafranov equations. However, an analytical solution (the Miller equilibrium) for the flux surface coordinates has been developed in terms of the elongation, triangularity and major radius of the displaced centers of the flux surfaces. The metrics for such a representation have been worked out, and the plasma fluid equations have been explicitly represented on this flux surface coordinate system, thus eliminating the need for a numerical solution to the Grad-Shafranov equation prior to solution of the transport equations in flux surface geometry.